PHYSICAL REVIEW D **80,** 015003 (2009)

Probing dark forces and light hidden sectors at low-energy e^+e^- colliders

Rouven Essig,[1] Philip Schuster,[1] and Natalia Toro[2]

[1]*Theory Group, SLAC National Accelerator Laboratory, Menlo Park, California 94025, USA*
[2]*Stanford Institute for Theoretical Physics, Stanford University, Stanford, California 94305, USA*

(Received 6 April 2009; published 6 July 2009)

A dark sector—a new non-Abelian gauge group Higgsed or confined near the GeV scale—can be spectacularly probed in low-energy e^+e^- collisions. A low-mass dark sector can explain the annual modulation signal reported by DAMA/LIBRA and the PAMELA, ATIC, and INTEGRAL observations by generating small mass splittings and new interactions for weak-scale dark matter. Some of these observations may be the first signs of a low-mass dark sector that collider searches can definitively confirm. Production and decay of $\mathcal{O}$(GeV)-mass dark states is mediated by a Higgsed Abelian gauge boson that mixes kinetically with hypercharge. Existing data from *BABAR*, BELLE, CLEO-c, and KLOE may contain thousands of striking dark-sector events with a high multiplicity of leptons that reconstruct mass resonances and possibly displaced vertices. We discuss the production and decay phenomenology of Higgsed and confined dark sectors and propose e^+e^- collider search strategies. We also use the DAMA/LIBRA signal to estimate the production cross sections and decay lifetimes for dark-sector states.

DOI: 10.1103/PhysRevD.80.015003 PACS numbers: 14.80.−j, 12.60.−i, 13.66.Hk, 95.35.+d

I. INTRODUCTION

Low-mass particles neutral under the standard model are nearly unconstrained by existing searches. We consider low-energy collider signatures of a new $\mathcal{O}$(0.1–10 GeV)-mass "dark" sector with gauge group G_D and light matter charged under it. The discovery of a dark sector that extends the structure of known low-energy gauge interactions would open a new frontier for particle physics and provide a second laboratory for fundamental questions including gauge unification and supersymmetry breaking.

If G_D contains an Abelian subgroup $U(1)_D$, high-scale physics generically induces kinetic mixing between the dark $U(1)_D$ and hypercharge, as sketched in Fig. 1; this mixing mediates direct production of dark-sector matter in high-luminosity scattering experiments. The decay of the dark-sector matter can lead to spectacular events with high lepton and hadron multiplicities, lepton pair masses reconstructing resonances in the dark sector, and possibly displaced vertices. In optimistic scenarios, thousands of these events could be sitting undiscovered in data collected by *BABAR*, BELLE, CLEO-c, and KLOE. Reconstructing new resonances in these events would reveal the dynamics of the dark sector.

Evidence for a low-mass dark sector is emerging from a surprising source: accumulating hints from terrestrial and satellite dark matter experiments indicate that dark matter is not an afterthought of the standard model's hierarchy problem, but instead has rich dynamics of its own. The local electron/positron excesses reported by HEAT [1], PAMELA [2,3], PPB-BETS [4], ATIC [5], and others [6,7] are suggestive of weak-scale dark matter interacting with a new light boson, for which the $U(1)_D$ is a natural candidate if its mass is $\mathcal{O}$(GeV). Dark-sector interactions can also generate the mass splittings among dark-matter states suggested by other experiments [8,9]. Dark matter scattering inelastically into an excited state split by $\mathcal{O}$(100 keV) can simultaneously explain the annual modulation signal reported by DAMA/NaI [10] and DAMA/LIBRA [11] and the null results of other direct-detection experiments [12,13]. Likewise, the INTEGRAL 511 keV excess at the Galactic center appears consistent with the excitation of dark matter states, but requires a slightly larger splitting of $\mathcal{O}$(MeV) [14,15].

The electron/positron excesses and the splittings suggested by the DAMA and INTEGRAL signals independently motivate an $\mathcal{O}$(GeV)-mass dark sector. If *any* of these anomalies are signals of dark matter, the new dynamics required to explain them can be discovered at e^+e^- colliders. Among the anomalies, DAMA's signal offers the most precise predictions for e^+e^- collider physics: the scattering rate is sensitive to the strength of kinetic mixing between the standard model and the dark sector, and gives reason to expect an observable direct production cross section for the dark sector.

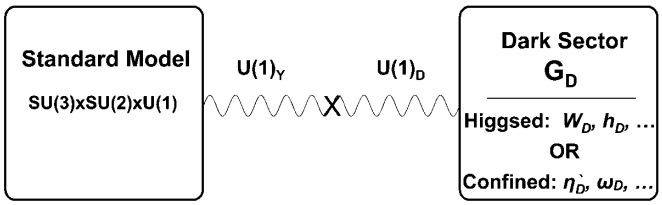

FIG. 1. We consider a dark sector with non-Abelian gauge group G_D, which is Higgsed or confined at $\mathcal{O}$(MeV–10 GeV). We assume that G_D contains a Higgsed Abelian factor $U(1)_D$, so that the dark sector interacts with standard model matter through kinetic mixing of hypercharge with the $U(1)_D$ gauge boson A', of mass in the same range. Either the Higgsed or confined phases of G_D necessarily include new states that can be produced through A' interactions.

A. Outline

In the remainder of this introduction, we further develop the motivation for a kinetically mixed light dark sector, and briefly describe the resulting events in low-energy e^+e^- collisions. In Sec. I B, we discuss the kinetic mixing that couples the standard model to the dark sector. In Sec. I C, we summarize the evidence that dark matter, with a mass of 100 GeV to 1 TeV, may interact with a low-mass dark sector. In particular, we introduce two frameworks for inelastic dark matter that motivate the Higgsed and confined dark sectors considered here. Though the dark matter in each model is heavy, in either case the generation of inelastic splittings requires *light* matter in the dark sector that can be produced at e^+e^- colliders. We describe the general structure of dark-sector production events in Sec. I D.

We then work our way into the dark sector, and back out. Two production modes are of interest, and their cross sections are nearly independent of the detailed structure of the dark sector. We present the production cross sections for general parameters in Sec. II A, and for the parameter ranges motivated by the inelastic dark matter models in Sec. II B. In Sec. III, we discuss the decay modes of metastable states, and the shapes of events expected within either Higgsed or confined dark sectors.

Section IV contains a brief discussion of search regions and strategies, which synthesizes the experimental consequences of the results of Sec. III. Section IV is self-contained, and readers who are not interested in the detailed decay phenomenology of different dark-sector models can skip Sec. III, and only read this section. We conclude in Sec. V.

Appendix A reviews the existing constraints on a new $U(1)_D$ gauge boson with mass $\mathcal{O}$(GeV) kinetically mixing with hypercharge. All numerical results are presented both for arbitrarily chosen fixed couplings, and for couplings normalized to the DAMA/LIBRA inelastic dark matter scattering cross section using the prescription in Sec. II B and Appendix B.

The B-factory phenomenology of pure $U(1)$ dark sectors has been discussed in [16], which notes a multi-lepton final state from a "Higgs-strahlung" process; and the phenomenology of MeV-scale dark-matter models in which $\gamma + e^+e^-$ or $\gamma +$ nothing final states dominate has been considered in [17]. The discussion of Sec. III is similar in spirit to the hadron collider phenomenology for hidden valleys [18–21] and the Higgsed dark-sector models discussed in [8,22,23] (see also [24]). Other work that discusses new physics beyond the standard model leading to rare Υ decays at low-energy e^+e^- colliders (albeit with very low-multiplicity or even no leptons in the final state), such as $\Upsilon \to \gamma +$ nothing, $\Upsilon \to$ invisible, or $\Upsilon \to \gamma H$ (where H is a light Higgs boson), includes [25–28].

B. $U(1)$ mixing with dark sectors

Any new Abelian gauge group $U(1)_D$ has a gauge-invariant kinetic mixing term with standard model hypercharge [29,30],

$$\Delta\mathcal{L} = \epsilon_Y F^{Y,\mu\nu} F^D_{\mu\nu}. \tag{1}$$

Several high-scale mechanisms, summarized below, generate $\epsilon_Y \sim 10^{-6}$–10^{-2} (we note that from string theory the range for ϵ_Y can be even larger [31]). Therefore, the setup illustrated in Fig. 1 is generic if there is any new gauge group containing a $U(1)_D$ factor.

The operator (1) is not generated at the Planck scale if $U(1)_Y$ is embedded in a grand unified theory (GUT), because it is not $SU(5)$ gauge-invariant. However, Planck-suppressed gauge-invariant operators involving GUT-breaking Higgses generate mixing

$$\epsilon_{\text{tree}} \sim \left(\frac{M_G}{M_{\text{Pl}}}\right)^p \tag{2}$$

when these Higgses obtain vacuum expectation values, where the power p depends on the representation content of the Higgses. For example, $p = 1$ for the operator $\frac{1}{M_{\text{Pl}}}\text{Tr}[\Phi F^5_{\mu\nu}]F_D^{\mu\nu}$, where Φ is an $SU(5)$ adjoint Higgs, and F^5 and F_D are the $SU(5)$ and dark-sector field strengths, respectively.

Kinetic mixing is also generated by heavy split multiplets charged under both $U(1)_D$ and $SU(5)$. Integrating out these multiplets generates loop-level mixing proportional to the logarithm of mass ratios within the multiplet:

$$\epsilon_{\text{loop}} \sim \frac{g_1 g_D}{16\pi^2} N_f \log\left(\frac{M}{M'}\right). \tag{3}$$

The mass splittings can themselves be generated by either tree- or loop-level effects, leading to ϵ_Y suppressed by one or two loop factors.

At low energies, the kinetic mixing can be removed by a field redefinition of $A^{Y,\mu}$, inducing ϵ-suppressed couplings of the A' to electromagnetically charged states,

$$\mathcal{L} \supset \epsilon g_D A'_\mu J^\mu_{\text{EM}}, \tag{4}$$

where $\epsilon \equiv \epsilon_Y \cos\theta_W$ and θ_W is the Weinberg weak mixing angle. Therefore, a light $U(1)_D$ gauge boson can and naturally does open a path into and back out of any dark sector.

C. Dark matter motivation for a *light* sector

Searches for a GeV-mass dark sector are particularly motivated by recent evidence for electroweak-mass dark matter with nontrivial structure. The consistency of *several* independent observations of distinct phenomena with the same qualitative framework is striking. Moreover, if any one of these observations is found to have a non-dark-matter origin, a low-mass dark sector is still strongly motivated by the other data.

Satellite observations and terrestrial experiments provide two kinds of evidence for a low-mass dark sector:

(1) Positron and/or electron flux measurements by PAMELA [2,3], PPB-BETS [4], and ATIC [5] point to an unknown local source of high-energy (100 GeV–TeV) electrons and positrons. If their source is dark matter annihilation or decay, synchrotron radiation from these electrons and positrons could also explain the WMAP haze near the Galactic center [32]. Two features of these experiments are suggestive of light states coupled to dark matter:

(i) The excess of electrons and positrons, without a visible antiproton excess [3], suggests dominantly leptonic decay or annihilation channels. One way to assure this is if the dark matter decays or annihilates into $\mathcal{O}$(GeV) particles that are kinematically forbidden from decaying to baryons [8].

(ii) If the excesses are produced by dark-matter annihilation, the annihilation cross section required to explain the signal is 10–1000 times larger than the thermal freeze-out cross section. This can be explained by Sommerfeld enhancement of the annihilation cross section through an $\mathcal{O}$(GeV) mass force mediator at low velocities [8].

(2) As we will discuss below, non-Abelian gauge interactions Higgsed or confined at the GeV scale can generate small mass splittings among states charged under them. Two observations suggest that dark matter may have such splittings:

(i) The INTEGRAL telescope [14] has reported a 511 keV photon signal near the Galactic center, indicating a new source of $\sim$1–10 MeV electrons and positrons. This excess could be explained by annihilation of light $\mathcal{O}$(1–10 MeV) dark matter [33], or by $\mathcal{O}$(100 GeV–1 TeV) dark matter with $\mathcal{O}$(MeV) excited states [15]. In the latter case, dark matter excited by scattering decays back to the ground state by emitting a soft e^+e^- pair.

(ii) The DAMA/NaI [10] and DAMA/LIBRA [11] experiments have reported an annual modulation signal over nearly 11 years of operation. Modulation is expected because the Earth's velocity with respect to the dark matter halo varies as the Earth moves around the sun, and the phase of the observed modulation is consistent with this origin. A simple hypothesis that explains the spectrum and magnitude of the signal, and reconciles it with the null results of other experiments, is that dark matter-nucleus scattering is dominated by an inelastic process,

$$\chi N \to \chi^* N, \tag{5}$$

in which the dark matter χ scatters off a nucleus N into an excited state χ^* with mass splitting $\delta \approx$ 100 keV [12].

Among these hints of new dark matter interactions, the inelastic dark matter (iDM) interpretation [12] of the DAMA/LIBRA signal deserves particular attention, because it is sensitive to the strength of coupling between the dark sector and the standard model. While the other data discussed above are consistent with extremely small kinetic mixing ϵ, the rate of scattering at DAMA/LIBRA fixes ϵ within a factor of few for fixed model parameters and A' mass, in a typical range $10^{-7} \lesssim \epsilon \lesssim 10^{-2}$. Therefore, the spectrum and rate of the signal reported by DAMA/LIBRA can be translated into predictions for the couplings of light states observable at e^+e^- colliders, as we will discuss below and in Sec. II B.

We summarize here how iDM reconciles the DAMA/LIBRA signal with null results from other searches. Inelastic scattering can only occur when the center-of-mass kinetic energy of the dark-matter-nucleus system exceeds the splitting δ. This implies that for a given target nucleus mass m_N and recoil energy E_R, the minimum lab-frame velocity of dark matter required for inelastic scattering is

$$\beta_{\min}(E_R) \simeq \frac{1}{\sqrt{2m_N E_R}}\left(\frac{m_N E_R}{\mu} + \delta\right), \tag{6}$$

where μ is the dark-matter-nucleus reduced mass. This energy threshold enhances the sensitivity of the DAMA/LIBRA experiment over other direct detection experiments in three ways:

(1) Dark matter with velocity below $v_{\min} \simeq \sqrt{2\delta/\mu}$ does not scatter. This minimum velocity increases for small m_N, thereby enhancing scattering off heavy nuclei such as iodine used in DAMA/LIBRA relative to scattering off silicon and germanium at CDMS [34].

(2) Dark matter direct searches obtain the tightest bounds on elastically scattering dark matter from low-energy nuclear recoils. If dark matter scatters inelastically, low-energy recoils require *higher* dark matter velocity, and are suppressed—see Eq. (6).

(3) The fraction of the halo velocity profile that exceeds $v_{\min} \simeq \sqrt{2\delta/\mu}$ is exponentially sensitive to changes in the Earth's velocity, leading to an $\mathcal{O}(1)$ annual modulation of the scattering rate, in contrast to the $\simeq$ 2–3% modulation typical of elastic scattering, which arises from the simple linear dependence of the dark matter flux on the Earth's velocity.

In this paper, we will consider dark-sector gauge groups Higgsed or confined at the GeV scale, both of which can generate $\mathcal{O}$(100 keV) splittings among $\mathcal{O}$(100 GeV–TeV) dark-matter states, with a kinetically mixed $U(1)_D$ mediating inelastic scattering off nuclei [8,9]. If the dark gauge group G_D contains a Higgsed non-Abelian factor, radiative effects can split all components of matter charged under G_D, with splittings

$$\delta \sim \alpha_D \Delta m_{W_D} \qquad \text{(Higgsed/radiative)}, \tag{7}$$

where Δm_{W_D} is a splitting of dark-sector gauge boson masses [8]. For example, $\Delta m_{W_D} \sim m_{W_D} \sim 1$ GeV and $\alpha_D \sim 10^{-4}$ gives $\delta \sim 100$ keV.

If instead a non-Abelian factor of G_D confines at a scale Λ_D, a heavy-flavor meson can be cosmologically long-lived and thus a dark matter candidate [9]. A particularly interesting limit for inelastic dark matter is when one dark quark is heavy ($m_{Q_D} \approx m_{\rm DM} \approx (100\ \text{GeV–}1\ \text{TeV}) \gg \Lambda_D$), and the other light ($m_{q_D} \lesssim \Lambda_D$). A cosmologically long-lived Q_D forms uncolored hadrons after confinement, of which the lightest, a spin-0 $Q_D \bar{q}_D$ meson, is a viable dark matter candidate. The spin-1 excited $Q_D \bar{q}_D$ meson is split by hyperfine interactions, which give

$$\delta \sim \frac{\Lambda_D^2}{N_C m_{\rm DM}} \qquad \text{(confined/hyperfine)}, \tag{8}$$

where N_C is the number of colors of G_D. For example, $m_{\rm DM} \sim 1$ TeV, $N_C = 3$, and $\Lambda_D \sim 500$ MeV gives $\delta \sim 100$ keV.

For both Higgsed and confined scenarios, the $U(1)_D$ described above in Sec. I B can mediate inelastic scattering of dark matter off standard model nuclei, with elastic scattering naturally suppressed. These mechanisms can also generate a splitting of $\mathcal{O}$(MeV) to explain the INTEGRAL excess [15].

Remarkably, though the mechanisms for generating the splitting from Higgsed and confined dark sectors are quite different, both are suggestive of dark sectors with multiple new states at $\mathcal{O}$(GeV)—precisely the range accessible in a variety of low-energy e^+e^- machines. In the Higgsed case, these states include gauge and Higgs bosons. In the confined case, these states include glueballs, light-flavor mesons, and baryons. Therefore, if either scenario is correct, experiments such as *BABAR*, BELLE, CLEO-c, and KLOE may be capable of discovering the kinds of spectacular events that we consider here.

We will see that the combination $\alpha_D \epsilon^2 / m_{A'}^4$, where $\alpha_D = g_D^2/4\pi$, determines the DAMA/LIBRA modulation rate. Therefore, we can use the observed modulation signal to estimate $\alpha_D \epsilon^2$ as a function of $m_{A'}$, which in turn determines the expected production cross section for $U(1)_D$-charged matter at e^+e^- colliders. We discuss this estimate in Sec. II B. The expected cross sections are $\mathcal{O}$(fb) for $m_{A'} \sim$ GeV. For heavier A', larger mixing parameters are required to reproduce the DAMA/LIBRA scattering rate; the resulting expected production cross sections scale as $\sim m_{A'}^4$. Therefore, very large cross sections are expected for a few-GeV A', while a dark sector with sub-GeV A' mass may evade detection in existing data.

D. Striking events at *B*-factories

Existing *B*-factory data sets, containing over 1.4 ab^{-1} of data altogether, are ideally suited to search for a dark $U(1)_D$ in the ~100 MeV–10 GeV mass range, and for any dark sectors they connect to. There are two leading production processes: an A' with mass beneath 10 GeV can be produced on-shell in association with a photon (the radiative return process). The A' initiates a cascade of dark sector decays if kinematically allowed; otherwise it decays to standard model fermions or hadrons. In addition, any light charged states within the dark sector can be produced through an off-shell A' carrying the full center-of-mass energy of the e^+e^- collision. The signatures of these processes are quite spectacular because decays or parton showers within the dark sector generate high particle multiplicities.

We focus on two cases, motivated by the dark matter models discussed in Sec. I C: a Higgsed dark sector containing only the non-Abelian gauge bosons and Higgses, and a confined sector with one light flavor.

In a Higgsed dark sector, the fate of the initially produced dark states is determined by spectroscopy: they decay to lower-mass states within the dark sector if such decays are kinematically accessible and allowed by symmetry. These cascades eventually produce light states that can only decay to standard model final states. Gauge boson decays are suppressed by two powers of the mixing parameter ϵ, and can be prompt or displaced. Higgs decays can be suppressed by ϵ^4, depending on kinematics, in which case they leave the detectors before decaying to visible matter. Typical events in a Higgsed dark sector can produce between 4 and 12 standard model particles, with leptons being a significant fraction and easiest to observe. Caricatures of these events, with and without a recoiling photon, are shown in Fig. 2. The decay phenomenology is similar in hadron colliders [21,23], and the pure Higgsed Abelian case for *B*-factories has been discussed in

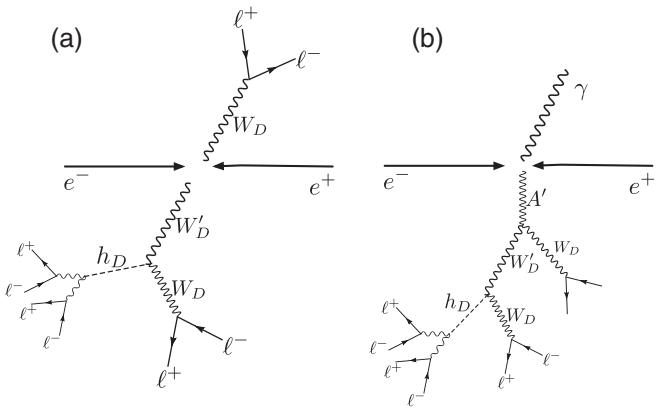

FIG. 2. Left: Cartoon of an event in which non-Abelian gauge bosons in a Higgsed dark sector are produced through an off-shell A': the gauge bosons may decay into other dark bosons (or fermions if present), which in turn decay to light standard model fermions. Right: a similar final state recoils off a hard photon in $A' + \gamma$ radiative return production.

[16], though the dominant production modes and kinematics considered here are quite different.

If the non-Abelian factor of G_D is confined, then the physical picture is very similar to the hidden valley models discussed in [18–20]. $U(1)_D$ mixing mediates production of a light quark-antiquark pair in the dark sector. These states shower and hadronize, producing few dark-sector mesons with a roughly spherical distribution if the ratio $\sqrt{s}/\Lambda_D$ is $\mathcal{O}(1)$, and collimated jets if this ratio is large. Unlike the Higgsed scenario, the multiplicity of mesons in a typical final state is determined by the ratio of the production energy to Λ_D, not by spectroscopy. Different scenarios are caricatured in Fig. 3. These sectors contain light mesons that can only decay to standard model final states. A single event can contain a combination of prompt and displaced decays, and states that escape the detector. In particular, dark pions that cannot decay within the dark sector are very long-lived because standard model matter is neutral under $U(1)_D$. This is quite different from the decays of hidden-valley pions, mediated by a Z' under which standard model matter and hidden-valley matter are both charged. Even when all states decay promptly, the reconstructed energy may still be less than the collider energy if some of the many tracks in these events are not reconstructed. Higgsed and confined-sector decays are discussed more carefully in Sec. III.

These considerations motivate searching for dark-sector events in *several* channels at e^+e^- colliders, as discussed in Sec. IV. We will argue that six qualitatively different searches cover a wide range of possible phenomenology:

(1) 4ℓ (exclusive), reconstructing $E_{\rm cm}$ (also $4\ell + \gamma$)
(2) 4ℓ (exclusive), with displaced dilepton vertices (also $4\ell + \gamma$)
(3) $\geq 5\ell$ + tracks (inclusive), reconstructing $E_{\rm cm}$ (also + γ)
(4) $\geq 5\ell$ + tracks (inclusive), with displaced dilepton vertices (also + γ)
(5) Very high track multiplicity, with many tracks consistent with leptons
(6) γ + nothing

The combined results of searches in these regions can discover or exclude kinetically mixed dark sectors over a wide range of mass scales and couplings, including much of the parameter region motivated by inelastic dark matter.

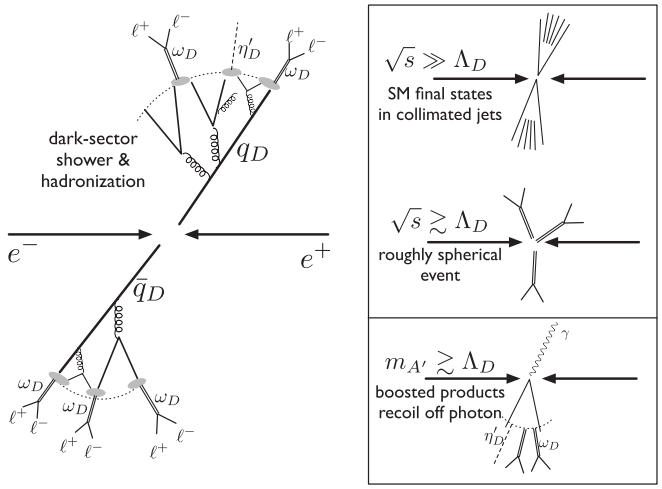

FIG. 3. Left: Cartoon of an event in which quarks in a simple confined dark sector are produced through an off-shell A'. The quarks shower and hadronize into mesons, which decay into standard model particles. Final states frequently contain many leptons, but can also include hadrons and long-lived dark states that escape the detector unobserved. Right: Phase space structure of different kinds of events. An off-shell A' produces jetlike structure if $\Lambda_D \ll \sqrt{s}$ (top), and approximately spherical final states if $\Lambda_D \lesssim \sqrt{s}$ (middle). In A'/γ radiative return production, the dark-sector final state recoils against a hard photon.

II. PRODUCTION MODES AND CROSS SECTIONS AT e^+e^- COLLIDERS

In this section, we discuss the production of dark-sector particles at e^+e^- colliders, with particular focus on the B-factories, *BABAR* and BELLE. The *BABAR* experiment at the SLAC National Accelerator Center collided e^+e^- pairs, obtaining 430 fb^{-1} of integrated luminosity on the $\Upsilon(4S)$ resonance, at a center-of-mass energy of 10.58 GeV. The Belle experiment at the KEK laboratory in Japan obtained an integrated luminosity of 725 fb^{-1} on the $\Upsilon(4S)$. The two experiments also acquired $\sim$270 fb^{-1} on the $\Upsilon(3S)$ and $\Upsilon(2S)$ resonances, and at nearby energies. The $\sim$1.4 ab^{-1} of data available to the two B-factories make these experiments ideally suited for searching for the $\mathcal{O}$(GeV) dark sectors suggested by direct detection and astrophysical data.

Over a large range of parameters, the cross sections for the production of dark-sector particles scale as

$$\sigma \sim \frac{\alpha \alpha_D \epsilon^2}{E_{\rm cm}^2}, \tag{9}$$

where $E_{\rm cm}$ is the center-of-mass energy of the collider, $\alpha_D = \frac{g_D^2}{4\pi}$, and g_D is the A' gauge coupling constant. The search sensitivity of a given e^+e^- machine above mass threshold scales as the ratio of integrated luminosity over squared center-of-mass energy, $\mathcal{L}_{\rm int}/E_{\rm cm}^2$. LEPI ($E_{\rm cm} \simeq$ 91 GeV and $\mathcal{L}_{\rm int} \sim 0.5$ fb^{-1}) and LEPII ($E_{\rm cm} \simeq$ 189–209 GeV and $\mathcal{L}_{\rm int} \sim 2.6$ fb^{-1}) are much less sensitive to direct production of low-mass dark sectors than the B-factories. As we will review below, however, searches for rare decays of the Z-boson can probe some of the relevant parameter space.

Compared to B-factories, lower-energy colliders such as DAΦNE, which runs at $E_{\rm cm} \simeq m_\Phi \simeq 1.02$ GeV, require much lower integrated luminosity to reach similar sensitivities to sub-GeV dark sectors. For example, the $\sim$2.5 fb^{-1} of data collected by KLOE at DAΦNE should

make this experiment competitive with any B-factory searches for sub-GeV mass dark sectors, though $\sim 1/3$ as many dark-sector events would be expected at DAΦNE than at BELLE. Importantly, the signatures of confined dark sector models can be quite different at $E_{\rm cm} \sim 10$ GeV compared to $E_{\rm cm} \sim 1$ GeV. Since there is less showering of dark sector states for lower $E_{\rm cm}$, events at KLOE may be easier to reconstruct than B-factory events. We will nevertheless concentrate on the B-factory phenomenology in this work, with the understanding that at least part of the discussion is qualitatively unchanged for several other e^+e^- colliders.

In Sec. II A, we quantitatively discuss the production modes and cross sections for general low-mass dark sectors coupled to the standard model sector via kinetic mixing. In Sec. II B, we will assume that stable matter in the dark sector explains the direct detection signal reported by DAMA/LIBRA, within the framework of inelastic dark matter. Under this assumption, we will estimate the expected production rates at B-factories from the direct detection rate reported at DAMA/LIBRA. Theoretically reasonable parameter ranges permit cross sections large enough to produce hundreds to tens of thousands of events at the B-factories.

A. Production processes for low-mass dark sectors

At e^+e^- colliders, there are two important dark-sector production modes. For definiteness, we focus here on the production of a pair of dark fermions, but the production cross section for a pair of dark gauge bosons in a Higgsed dark sector, which occurs through mass mixing of the A' with non-Abelian gauge bosons, is similar.

We first consider the direct production of a pair $X\bar{X}$ of dark-sector fields through an off-shell A', shown in Fig. 4(a). The cross section for this off-shell production process is

$$\sigma_{X\bar{X}} = N_c \frac{4\pi}{3} \frac{\epsilon^2 \alpha \alpha_D}{E_{\rm cm}^2} \left| 1 - \frac{m_{A'}^2}{E_{\rm cm}^2} - \frac{i m_{A'} \Gamma}{E_{\rm cm}^2} \right|^{-2} \times \sum_{i=1}^{N_f} q_i^2 \sqrt{1 - \frac{4m_{X_i}^2}{E_{\rm cm}^2}} \left(1 + \frac{2m_{X_i}^2}{E_{\rm cm}^2}\right) \simeq 0.78 \text{ fb} N_c \left(\frac{\epsilon}{10^{-3}}\right)^2 \left(\frac{\alpha_D}{\alpha}\right) \left(\frac{E_{\rm cm}}{10.58 \text{ GeV}}\right)^{-2} \times N_f. \tag{10}$$

Here, N_c is the number of colors in the dark sector gauge group G_D, N_f is the number of dark sector particles X_i coupling to A' with charges q_i, and the other variables were defined in Eq. (9). This cross section is nonzero even for $m_{A'}$ much larger than $E_{\rm cm}$, as long as $m_X < E_{\rm cm}/2$.

The second production mode, shown in Fig. 4(b), is that of an on-shell A' and a photon, with differential cross section

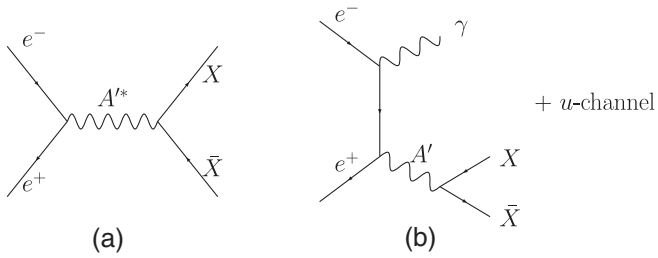

FIG. 4. Production modes of light dark-sector particles $X\bar{X}$ at B-factories. (a) Production through an off-shell A'. (b) Production of an on-shell A' and a photon—we assume the A' subsequently decays into lighter dark-sector particles.

$$\frac{d\sigma_{\gamma A'}}{d\cos\theta} = \frac{2\pi\epsilon^2\alpha^2}{E_{\rm cm}^2}\left(1 - \frac{m_{A'}^2}{E_{\rm cm}^2}\right)\frac{1 + \cos^2\theta + \frac{4m_{A'}^2/E_{\rm cm}^2}{(1 - m_{A'}^2/E_{\rm cm}^2)^2}}{(1 + \cos\theta)(1 - \cos\theta)}, \tag{11}$$

where θ is the angle between the beam line and the photon momentum. This has singularities as the photon becomes collinear with the initial-state electron or positron. The singularity is cut off by the electron mass, but if we demand that the photon be detected in the electromagnetic calorimeter in the range $\cos\theta_{\rm min} < \cos\theta < \cos\theta_{\rm max}$, the cross section is

$$\sigma = \frac{2\pi\epsilon^2\alpha^2}{E_{\rm cm}^2}\left(1 - \frac{m_{A'}^2}{E_{\rm cm}^2}\right)\left(\left(1 + \frac{2m_{A'}^2/E_{\rm cm}^2}{(1 - m_{A'}^2/E_{\rm cm}^2)^2}\right)\Theta - \cos\theta_{\rm max} + \cos\theta_{\rm min}\right) \tag{12}$$

$$\sim 2.4 \text{ fb}\left(\frac{\epsilon}{10^{-3}}\right)^2\left(\frac{E_{\rm cm}}{10.58}\right)^{-2}\left(\log\frac{4}{\theta_{\rm min}(\pi - \theta_{\rm max})} - 1\right), \tag{13}$$

where

$$\Theta \equiv \log\left(\frac{(1 + \cos\theta_{\rm max})(1 - \cos\theta_{\rm min})}{(1 + \cos\theta_{\rm min})(1 - \cos\theta_{\rm max})}\right) \approx 6 \tag{14}$$

is an enhancement from the t-channel singularity (the numerical estimate is obtained from the *BABAR* calorimeter range in the center-of-mass frame, $-0.92 \lesssim \cos(\theta_{\rm min}) \lesssim 0.87$ [35]), and we assume $m_{A'}^2 \ll E_{\rm cm}^2$ in Eq. (13). The on-shell process (13) is enhanced by $\sim \frac{\alpha}{\alpha_D}\Theta$ relative to the off-shell mode (10).

For $m_{A'} \sim 1$ GeV, $\alpha_D = \alpha$, and $\epsilon = 10^{-3}$, the relevant cross sections are $\mathcal{O}$(fb) at the B-factories. With a total integrated luminosity of ~ 1.4 ab^{-1}, this corresponds to several hundred to a few thousand dark-sector production events! In Fig. 5, we show the inclusive cross sections at the B-factories for off-shell and on-shell production of dark-sector particles as a function of either $\alpha_D\epsilon^2$ or ϵ^2 and $m_{A'}$. Figure 6 shows a similar plot for DAΦNE.

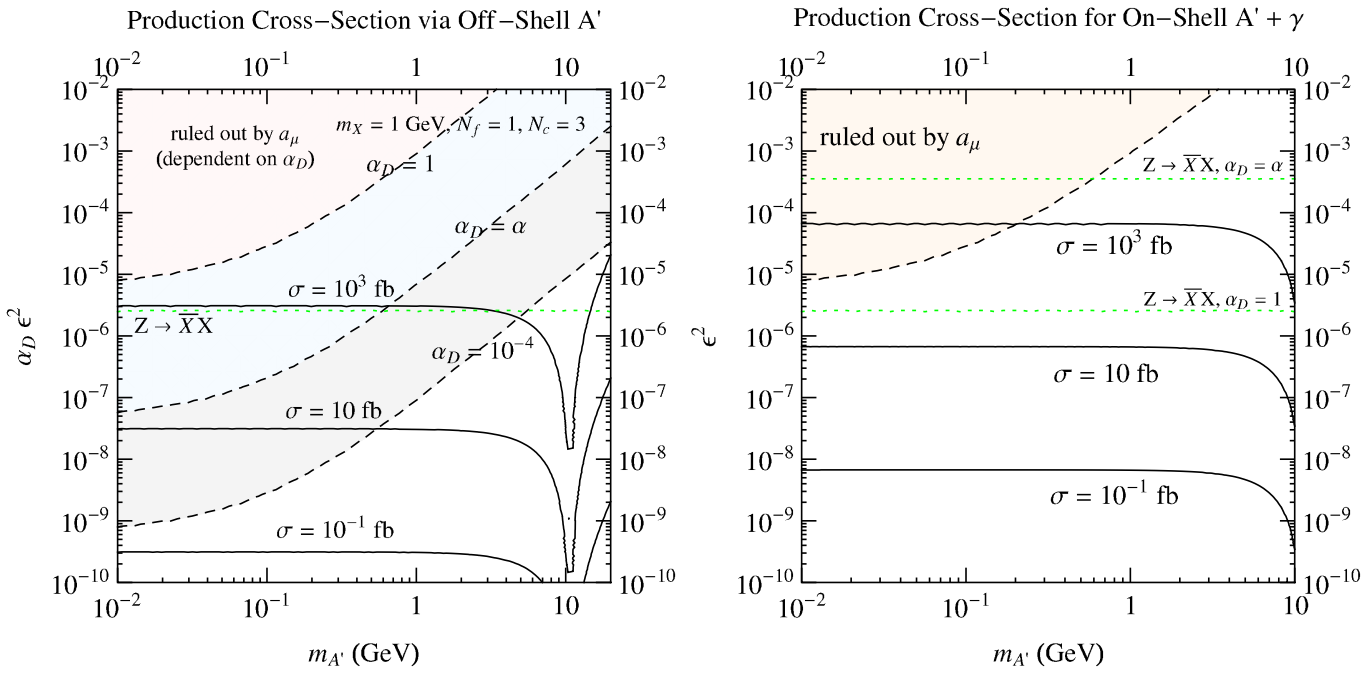

FIG. 5 (color online). Left: Inclusive cross section at the B-factories ($E_{\rm cm} = 10.58$ GeV) for production of dark-sector states X via an off-shell A' as a function of $\alpha_D\epsilon^2$ and $m_{A'}$, for $m_X = 1$ GeV, $N_f = 1$, $N_c = 3$, and unit charges q_i [Eq. (10)]. Note that the cross section scales linearly with the number of dark flavors N_f and dark colors N_c. Right: Cross section at the B-factories for production of an on-shell A' and a photon as a function of ϵ^2 and $m_{A'}$ [Eq. (12)]. Black lines correspond to fixed cross sections. Also shown are the constraints on the couplings of a new $U(1)_D$ mixing with hypercharge from measurements of the muon anomalous magnetic dipole moment (shaded regions) [36]. The green dotted lines correspond to the lower bounds on the range of couplings that could be probed by a search at LEPI for rare Z-decays to various exotic final states, assuming that branching ratios as low as 10^{-5} can be probed. More details are given in Appendix A.

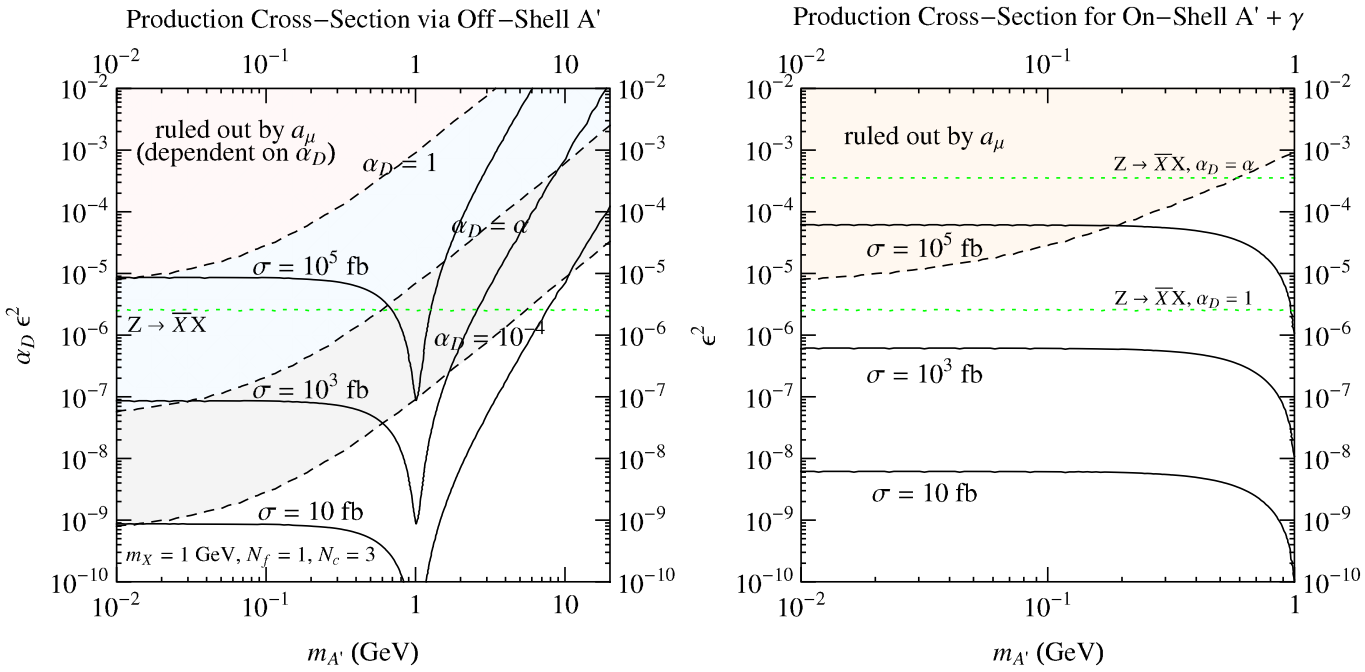

FIG. 6 (color online). As in Fig. 5, but for the center-of-mass energy of DAΦNE ($E_{\rm cm} = 1.02$ GeV).

Figures 5 and 6 also show constraints on the couplings of a new $U(1)_D$ mixing with hypercharge. Shown in shaded regions are constraints derived from the muon anomalous magnetic dipole moment a_μ as in [36]. The measured value of a_μ is larger than the theoretically predicted value, based on e^+e^- annihilation to hadrons, by $(302 \pm 88) \times 10^{-11}$ [37,38], and the constraints shown assume that the contribution from loops of the A' to a_μ is smaller than $(302 + 5 \times 88) \times 10^{-11}$. This constraint is discussed in more detail in Appendix A.

Since any mixing between $U(1)_D$ and $U(1)_Y$ induces a coupling between Z-bosons and matter in the dark sector, decays $Z \to X\bar{X}$ are possible. Depending on the decay modes of X, which we will discuss in detail in Sec. III, a variety of signatures is possible. For example, if the X's decay invisibly or outside the detector, the constraint is not better than the uncertainty on the width of the Z, which is about 0.1%. More exotic Z decays into multileptons are possible, but require dedicated searches. The best constraints on rare Z decay branching ratios are no better than the 10^{-6}–10^{-5} level [39], and even dedicated searches may not reach this level for complicated final states. In Figs. 5 and 6, we show (green dotted lines) the value of $\alpha_D\epsilon^2$ corresponding to a branching ratio of $Z \to X\bar{X}$ as small as 10^{-5}. The potential reach of rare Z-decay searches is discussed in more detail in Appendix A.

Finally, we mention two collider constraints on the production cross section which are only relevant for certain decay modes. The first one is from the CLEO Collaboration which searched for decays $\Upsilon(1S) \to \gamma$ + nothing [40]. This is relevant for the case when the X's are long-lived and decay outside the detector. As we will see in Secs. III and IV, this is a very important search mode. Using an integrated luminosity of 48 pb^{-1} of data, CLEO found no peak in the photon energy in the range 1–4.7 GeV [40]. The resulting limit can be interpreted as excluding cross sections as low as 200–500 fb, depending on the A' mass, though [40] assumes a different photon angular distribution than would result from dark-sector production.

The second collider constraint comes from a search for $\Upsilon(3S) \to \gamma A' \to \gamma\mu^+\mu^-$ by the *BABAR* Collaboration [41], which is only relevant if A' decays to dark-sector particles are kinematically forbidden, in which case it decays to standard model states. In 30 fb^{-1} of data containing $\sim 122 \times 10^6$ $\Upsilon(3S)$ events, a 90% C.L. upper limit of roughly 4×10^{-6} on the $\gamma\mu^+\mu^-$ branching fraction was found for $m_{A'}$ of a few hundred MeV. This search would also be sensitive to about $500\gamma\mu^+\mu^-$ events through A'/γ production. In this mass range, $\text{Br}(A' \to \mu^+\mu^-) \approx 0.3$–$0.5$ [39]. These results exclude production of about $1000\gamma A'$ events, corresponding to a cross section of about 30 fb. For A' masses of a few GeV, but below the τ threshold, the limits exclude $250\gamma\mu^+\mu^-$ events, but $\text{Br}(A' \to \mu\mu) \approx 0.2$–$0.25$ so that a similar cross section limit is obtained. We note that even if the A' is the lightest state of the dark-sector, any other kinematically accessible states are pair-produced with a comparable rate through an off-shell A', which produces a signal in the multilepton channel (see Sec. III), which has much lower QED backgrounds. Lower cross sections can thus be probed by considering different final states.

In summary, the potential search mode for rare Z decays and the a_μ constraint do not exclude parameter regions in which thousands of events could be seen. Collider searches for γ + nothing and $\gamma + \mu^+\mu^-$ final states have probed some of this parameter space, but are quite model-dependent. More general final states could easily have been missed by existing searches, even if they occur with large cross sections.

Before discussing the decay of X's in Sec. III, we use the hypothesis that an $\mathcal{O}(100\ \text{GeV})$ stable particle charged under G_D explains the direct detection signal reported by DAMA/LIBRA. We use this to estimate the dark-sector couplings $\alpha_D\epsilon^2$ and resulting production cross sections of low-mass dark sector states at B-factories.

B. Inelastic dark matter and inclusive cross sections

Inelastic dark matter (iDM) can reconcile the annual modulation signal reported by the DAMA/LIBRA Collaboration with the null results of other experiments [12,13]. In proposals to generate the iDM splitting from new non-Abelian gauge interactions in a ~GeV-mass dark sector, it is also natural to assume that scattering is mediated by a $U(1)_D$ gauge boson A' that mixes kinetically with the photon, with mass $m_{A'}$ of $\mathcal{O}(100\ \text{MeV}$–$10\ \text{GeV})$ [8]. In such models, the signal rate and spectrum reported by DAMA/LIBRA constrain the couplings of the A' to the standard model electromagnetic current. This allows us to estimate the inclusive cross section for production of dark states at B-factories for a given iDM model.

At energies beneath $m_{A'}$, the dark matter interacts with charged matter through an effective coupling

$$\mathcal{L} \simeq \frac{e g_D \epsilon}{m_{A'}^2} J^\mu_{\text{EM}} J_{\mu,\text{Dark}}, \tag{15}$$

where $J_{\mu,\text{Dark}}$ is a current composed of dark sector fields, and e and g_D are the photon and A' coupling strengths, respectively. The combination $\frac{\alpha_D\epsilon^2}{m_{A'}^4}$ ($\alpha_D = g_D^2/4\pi$) controls the scattering rate of dark matter in direct detection experiments (see Appendix B), while $\alpha_D\epsilon^2$ determines the inclusive production cross section at B-factories. Consequently, the production cross section can be estimated as a function of $m_{A'}$.

We will consider two classes of iDM theories—one where the dark matter is directly charged under the $U(1)_D$ [8], and one where the dark matter is a neutral composite meson, built out of charged spin-1/2 constituents, one of which is light (~ GeV) and the other heavy ($m_{\text{DM}} \sim 100$–1000 GeV) [9]. Higgsed dark sectors are an

example of the first class of theories, in which the breaking of the dark gauge group generates mass splittings for the dark matter gauge eigenstates. The resulting mass eigenstates couple off-diagonally to the A', leading to inelastic scattering. The low-energy scattering matrix elements are

$$\langle \chi^*(p')|J^\mu_{\rm Dark}|\chi(p)\rangle_{\rm Charged\ Scattering} = (p + p')^\mu, \quad (16)$$

where we have neglected higher order spin-dependent terms. Confined dark sectors are an example of the second class of theories, in which hyperfine interactions among the constituents split the ground state meson into a pseudoscalar and vector [9]. If the $J^\mu_{\rm Dark}$ coupling breaks parity, then the leading scattering operators mediate inelastic hyperfine transitions (dipole scattering) with matrix elements

$$\langle \chi_V(p', \epsilon^\mu)|J^\mu_{\rm Dark}|\chi_S(p)\rangle_{\rm Dipole\ Scattering} \approx \frac{c_{\rm in}}{\Lambda_D}(p + p')^\mu \epsilon \cdot q, \quad (17)$$

where ϵ^μ is the polarization of the outgoing χ_V and $q = p - p'$ is the momentum transfer. The natural magnitude of the dipole moment $b = \frac{c_{\rm in}}{\Lambda_D} \sim {\rm GeV}^{-1}$ is the size Λ_D^{-1} of the composite dark matter (Λ_D is of order the confining scale of the dark gauge group). Relative to the charged scattering matrix element (16), this scattering is suppressed by a q-dependent form factor.

For either current, the cross section to scatter off of a nuclear target of mass m_N and charge Z with recoil energy E_R is

$$\frac{d\sigma}{dE_R} \approx \frac{8\pi Z^2 \alpha \alpha_D \epsilon^2 m_N}{v^2(2m_N E_R + m_{A'}^2)^2}|F(E_R)|^2 \begin{cases} 1 & \text{(charged(vector-current))} \\ \frac{c_{\rm in}^2}{2}\frac{m_N E_R}{\Lambda_D^2} & \text{(form-factor(dipole))}, \end{cases} \quad (18)$$

where $\alpha = \frac{e^2}{4\pi}$, v is the dark matter-nucleus relative velocity, and $F(E_R)$ is a nuclear form factor. As discussed in Appendix B, we compute the scattering rate from Eqs. (16) and (17), fit the reported DAMA/LIBRA rate, and thereby obtain an estimate for the couplings $\alpha_D\epsilon^2$ as a function of $m_{A'}$.

From Eq. (18), we see that the dipole scattering cross section is a function of the momentum-dependent form factor $\frac{m_N E_R}{\Lambda_D^2} \sim \frac{q^2}{\Lambda_D^2}$. To estimate the coupling $\alpha_D\epsilon^2$ for a given $m_{A'}$, we must thus choose a value for Λ_D. Λ_D can in principle be determined by fitting δ to the DAMA/LIBRA data, since δ is proportional to $\Lambda_D^2/m_{\rm DM}$. However, the constant of proportionality is model-dependent. Following [9], we introduce a scale $\tilde{\Lambda}_D$, such that

$$\delta \equiv \frac{\tilde{\Lambda}_D^2}{m_{\rm DM}}. \quad (19)$$

In general,

$$\tilde{\Lambda}_D \sim \begin{cases} \frac{\Lambda_D}{\sqrt{N_c}} & \text{(strong coupling)} \\ \alpha' \Lambda_D & \text{(coulomb regime)}, \end{cases} \quad (20)$$

where the first case corresponds to a heavy meson of a $SU(N_c)$ confining at Λ_D, and the second case corresponds to a meson in a weak-coupling coulomb regime with coupling α'. $\tilde{\Lambda}_D/\Lambda_D$ is naturally a small number in either

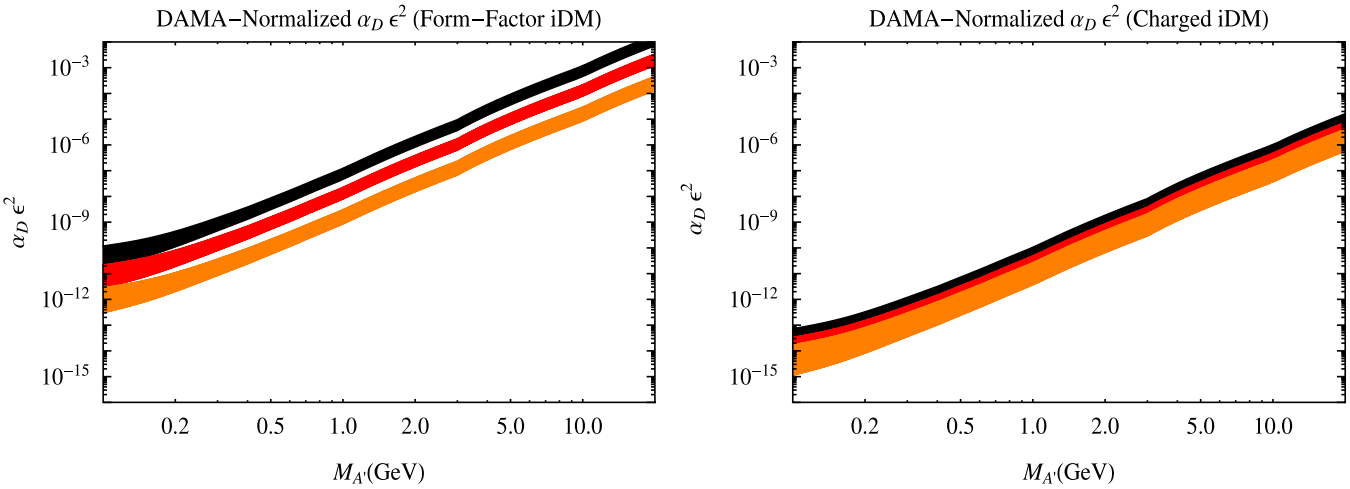

FIG. 7 (color online). $\alpha_D\epsilon^2$ as a function of $m_{A'}$, normalized to the DAMA/LIBRA annual modulation signal. Black, red, and orange bands from top to bottom correspond to $m_{\rm DM} = 2000$, 800, and 200 GeV, respectively. Uncertainties in fitting to DAMA/LIBRA, as a function of the inelastic dark matter mass splitting, are reflected in the thickness of the bands. The left plot shows the normalized couplings for inelastic dark matter that scatters via form-factor-suppressed dipole scattering [Eq. (17)], typical for a confined dark sector, with $\tilde{C} = 0.01$ ($\alpha_D\epsilon^2$ scales as $1/\tilde{C}$). The right plot shows the normalized couplings for charged scattering (Eq. (16)], which is typical for a Higgsed dark sector.

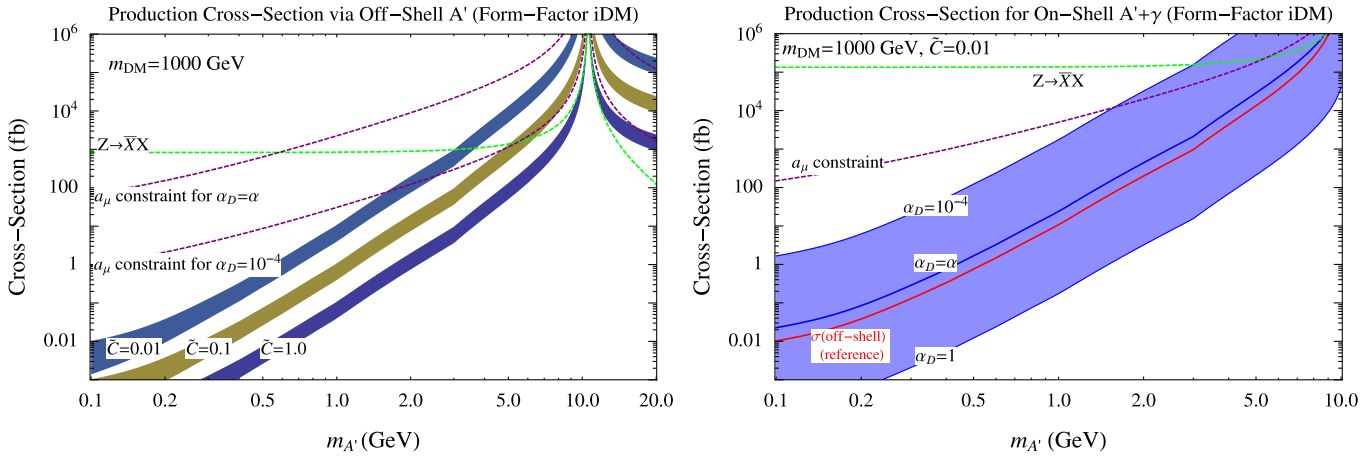

FIG. 8 (color online). Inclusive cross section at the B-factories for production of dark-sector states X through an off-shell A' (left) and for production of an on-shell A' with a photon (right) as a function of $m_{A'}$, after normalizing to the observed DAMA/LIBRA modulation rate assuming form-factor-suppressed dipole inelastic dark matter scattering. We set $m_{\rm DM} = 1$ TeV. In the left plot, we set $m_X = 1$ GeV, $N_f = 1$, $N_c = 3$, $q_i = 1$, and show various choices of $\tilde{C} = \{0.01, 0.1, 1.0\}$, while in the right plot, we show $\alpha_D = \{1, \alpha, 10^{-4}\}$ with $\tilde{C} = 0.01$. Note that the off-shell production cross section scales linearly with the number of dark flavors N_f and dark colors N_c. Also shown on both plots are constraints from a_μ as well as the rare Z-decay sensitivity region—see Appendix A for more details.

case. We absorb the uncertainty in both Λ_D and $c_{\rm in}$ in a single proportionality factor

$$\tilde{C} \equiv \left(\frac{c_{\rm in}^2 \tilde{\Lambda}_D^2}{\Lambda_D^2}\right), \tag{21}$$

which is naturally small ($\tilde{C} \sim 0.01$–1). The dark matter scattering rate is now exactly fixed by the inelastic splitting δ and $\tilde{C}$, allowing the determination of $\alpha_D \epsilon^2$ from the DAMA/LIBRA scattering rate as a function of $m_{A'}$. For the charged scattering (16), there is no analogous unknown parameter, and we can solve for $\alpha_D \epsilon^2$ directly from (18).

Figure 7 shows the DAMA/LIBRA-normalized couplings as a function of $m_{A'}$ for charged and dipole scattering, and for different dark-matter masses. In Fig. 8, we show the B-factory cross sections using dark-sector couplings normalized for dipole scattering. In Fig. 9, we show cross sections normalized using charged scattering. For $m_{A'} \geq 100$ MeV, B factory cross sections are expected to easily exceed $\sim$1 fb for composite iDM theories. For theories where the iDM scattering is charged-current dominated, $\sim$1 fb cross section can occur for $m_{A'} \geq 1$ GeV. In general, the estimated cross sections scale as $m_{A'}^4$.

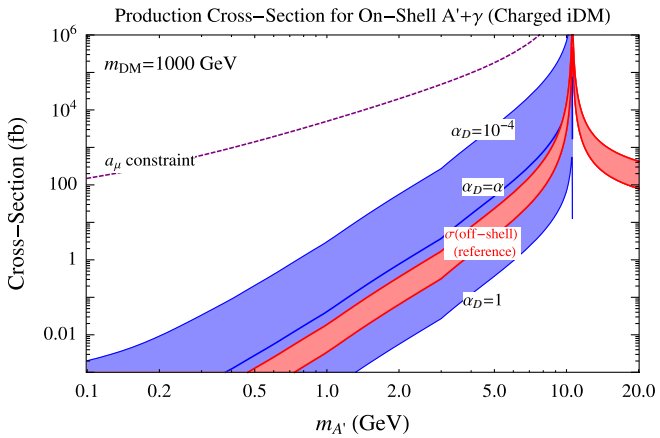

FIG. 9 (color online). As in Fig. 8, but here the production cross sections are normalized to the observed DAMA/LIBRA modulation rate assuming charged inelastic dark matter scattering.

We note that the e^+ and/or e^- data from, for example, PAMELA, ATIC, and PPB-BETS cannot be used in the same way as the DAMA data to predict the cross sections at low-energy e^+e^- colliders. The reason is that the e^+ and/or e^- data do not directly constrain the A' coupling with the electromagnetic current. Since the dark matter annihilates into *on-shell* A''s that decay with a lifetime that is largely unconstrained by the data, the mixing parameter ϵ is also unconstrained. However, indirect constraints on the dark matter annihilation cross section from, for example, γ-ray observations [42,43], and cosmic microwave background measurements [44] constrain the maximum allowable Sommerfeld enhancement, and currently disfavor very low A' masses ($\sim$ 100 MeV or less).

III. DECAYS OF DARK-SECTOR STATES INTO STANDARD MODEL PARTICLES

In this lengthy section, we discuss the decays of dark-sector states produced at e^+e^- colliders. Readers interested in the experimental consequences of these decays can skip to Sec. IV, which is self-contained.

The kinetic mixing that allows dark-sector states to be produced at e^+e^- colliders also allows them to decay back into standard model states, mainly leptons and light hadrons. To demonstrate the range of phenomenology possible

in both Higgsed and confined dark sectors, we have considered several kinematic limits that exhibit different properties. We will also briefly consider the impact of Higgs mixing on decays. We organize our discussion around the following questions:

(1) What are the metastable states of the dark sector that can *only* decay through processes that involve kinetic mixing?
(2) What are the decay widths of these metastable states?
(3) What are the multiplicities and kinematic properties of these metastable states?

We consider Higgsed dark sectors in Sec. III A and confined dark sectors in Sec. III B. In both cases, decays of spin-1 states through A' mixing, suppressed by ϵ^2, are generically prompt, while other species can have displaced 3-body decays or invisible decays suppressed by ϵ^4. Therefore, different dark-sector spectra can give rise to very different phenomenology, with all dark-sector states decaying promptly into the standard model, all states so long-lived that they escape the detector, or a combination of prompt, displaced, and/or invisible decays. Light fermions in the dark sector lead to events with more invisible decay products, as we discuss in Sec. III C.

Through most of this discussion we consider only the decays generated by the A'/γ kinetic mixing, but other interactions between the standard model and dark sector, involving either standard model Higgs bosons or new heavy fields coupled to both sectors, are also possible. Though these have no observable effect on direct production, they can dominate over the kinetic-mixing-induced decay modes that scale as ϵ^4. These interactions could be discovered through the observation of displaced decays that are *not* induced by kinetic mixing—specifically, a two-fermion decay of spin-0 states (Sec. III A 3) and any decay of the lightest dark-sector fermion (Sec. III C).

A. Events from a Higgsed dark sector

We assume that the dark sector gauge group G_D has been completely Higgsed, giving mass to all dark-sector gauge bosons. We also assume that all custodial symmetries have been broken, so that couplings $W_iW_jW_k$, $W_iW_jh_k$, and $W_ih_ih_j$ are generated between all Higgs and gauge bosons. The custodial symmetry breaking ensures that the A' mediates inelastic transitions between the dark matter and its excited states, which is needed to explain the DAMA/LIBRA and INTEGRAL signals [8,23]. As all mass eigenstates are mixed, we will not distinguish between the Abelian gauge boson A' and non-Abelian gauge bosons, but refer to all as W_D.

The high-energy collider phenomenology of these models has been discussed in [23], and many of the same features control low-energy collider signatures as well. The special case of a pure $U(1)$ dark sector was recently discussed in [16]. In Sec. III A 1, we determine the metastable states and their decays mediated through kinetic mixing. We discuss the final-state multiplicities in Sec. III A 2. In Sec. III A 3, we comment on other interactions that induce faster decays than those mediated by kinetic mixing.

1. Metastable states and their decays through kinetic mixing

We begin with a somewhat careful discussion of the metastable states—those that can only decay through kinetic mixing to standard model states, or equivalently those whose lifetimes vanish in the $\epsilon \to 0$ limit. States that can decay to final states within the dark sector are *not* considered metastable, and these decays are typically prompt. The standard model states produced in the decay of metastable states include mainly leptons and pions. We denote the mass of the lightest dark-sector gauge boson by $m_{W_{D,\min}}$, and the mass of the lightest Higgs by $m_{h_{D,\min}}$. Any Higgs heavier than $2m_{W_{D,\min}}$ can decay to two gauge bosons, and any W_D heavier than $2m_{h_{D,\min}}$ can decay to two Higgses. Therefore, if $m_{h_{D,\min}} > 2m_{W_{D,\min}}$, only W_D's are metastable; if $m_{W_{D,\min}} > 2m_{h_{D,\min}}$, then only Higgses are metastable. More than one dark gauge or Higgs boson may be metastable in each case, but they will decay similarly. If $\frac{1}{2}m_{W_{D,\min}} < m_{h_{D,\min}} < 2m_{W_{D,\min}}$, then the dark sector contains at least one metastable Higgs, and at least one metastable gauge boson.

The importance of this characterization is that the gauge and Higgs bosons have very different lifetimes: gauge bosons typically decay promptly, while Higgs decays give rise to displaced decays or escape the detector before decaying. A typical dark-sector production event will eventually decay to a collection of metastable states, consisting either of only Higgs bosons, only gauge bosons, or a combination of both. This leads to a variety of scenarios with very different decay phenomenology, summarized in Fig. 10. In the following, we justify the decay properties claimed in that figure.

If W_D's are metastable, they can decay to standard model leptons and pions through kinetic mixing. By assumption, all gauge bosons have some mixing angle θ with $U(1)_D$, giving rise to a decay width

$$\Gamma(W_D \to \ell^+\ell^-) = \frac{1}{3}\epsilon^2\theta^2\alpha m_{W_D}\sqrt{1-\frac{4m_\ell^2}{m_{W_D}^2}}\left(1+\frac{2m_\ell^2}{m_{W_D}^2}\right)N_{\text{eff}}$$
$$\simeq 2.4\ \text{eV}\left(\frac{\epsilon}{10^{-3}}\right)^2\theta^2\left(\frac{m_{W_D}}{1\ \text{GeV}}\right)\times\sqrt{1-\frac{4m_\ell^2}{m_{W_D}^2}}\left(1+\frac{2m_\ell^2}{m_{W_D}^2}\right)N_{\text{eff}}, \qquad (22)$$

where m_ℓ denotes the mass of a lepton *or* a hadron. Here N_{eff} counts the number of available decay products: $N_{\text{eff}} = 1$ for $m_{W_D} \lesssim 2m_\mu$ when only $W_D \to e^+e^-$ decays are

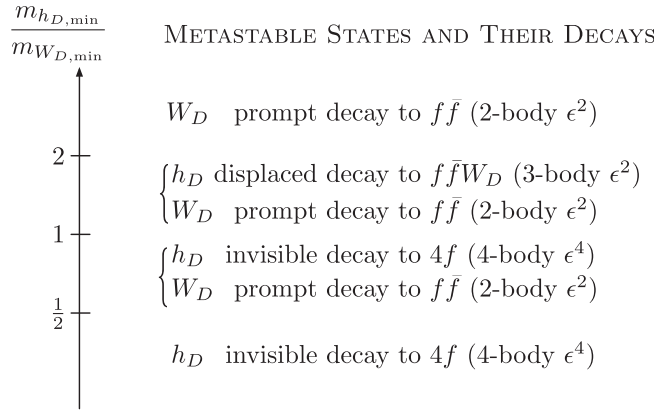

FIG. 10. Summary of decay phenomenology in Higgsed dark sectors. While decays within the dark sector are prompt, the lightest dark-sector state can only decay into standard model leptons or hadrons with a width that is suppressed by some power of ϵ. Generically, this decay is prompt if the lightest state is a gauge boson, while it is displaced or invisible if it is a Higgs. The figure summarizes the decay phenomenology as a function of the mass ratio of the lightest Higgs boson to the lightest gauge boson $\frac{m_{h_{D,\min}}}{m_{W_{D,\min}}}$.

possible, and $2 + R(m_{W_D})$ for $m_{W_D} \geq 2m_\mu$, where R is defined to be the energy-dependent ratio $\sigma(e^+e^- \to \text{hadrons})/\sigma(e^+e^- \to \mu^+\mu^-)$ [39].

The decay length of W_D in its rest frame is given by

$$c\tau(W_D \to \ell^+\ell^-) \sim 8 \times 10^{-6}\ \text{cm}\left(\frac{10^{-3}}{\epsilon}\right)^2 \theta^{-2}\left(\frac{1\ \text{GeV}}{m_{W_D}}\right) \times \left(\frac{1}{N_{\text{eff}}}\right), \tag{23}$$

and is thus prompt for $\theta \sim \mathcal{O}(1)$. The combination $\alpha_D\epsilon^2$ can also be normalized to its DAMA/LIBRA expected value. In this case,

$$c\tau(W_D \to \ell^+\ell^-) \sim 10^{-3}\ \text{cm}\theta^{-2}\left(\frac{1\ \text{GeV}}{m_{W_D}}\right)\left(\frac{1\ \text{GeV}}{m_{A'}}\right)^4\left(\frac{\alpha_D}{\alpha}\right) \times \left(\frac{1\ \text{TeV}}{m_{\text{DM}}}\right)\left(\frac{1}{N_{\text{eff}}}\right), \tag{24}$$

where m_{DM} is the mass of the dark matter (see Sec. II B). We see that prompt decays are also generic. However, due the strong dependence of $c\tau$ on $1/m_{A'}^4$, displaced vertices are also possible for $m_{A'} \sim \mathcal{O}(100\ \text{MeV})$.

If Higgses are metastable, they can decay to standard model leptons and hadrons through one or two off-shell W_D's (heavier Higgses can have 3-body decays to a lighter Higgs and $W_D^* \to \ell^+\ell^-$). If $m_{h_D} > m_{W_{D,\min}}$, one final-state W_D can be on-shell, and the lifetime is

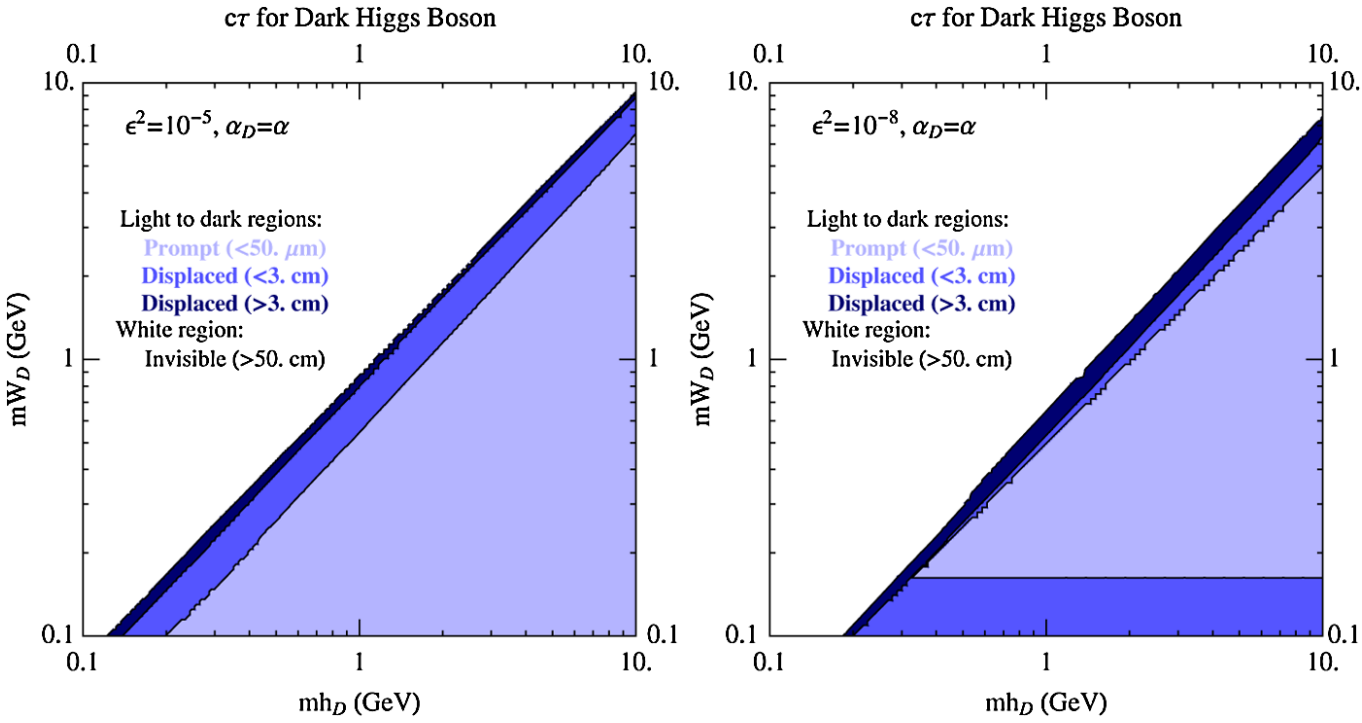

FIG. 11 (color online). Decay length ($c\tau$) of a dark-sector Higgs boson $h_D \to W_iW_j^* \to W_i\ell\ell$ as a function of its mass m_{h_D} and the dark-sector gauge boson mass m_{W_D}, for $\alpha_D = \alpha$ and $\epsilon = 10^{-5}$ (left) and $\epsilon = 10^{-8}$ (right). Here ℓ denotes a standard model lepton or hadron. The light to dark (light-blue/blue/dark-blue) regions indicate decays that are prompt ($< 50\ \mu$m), short displaced (< 3 cm), and long displaced (> 3 cm), while in the white region the decays are invisible (> 50 cm).

$$\Gamma(h_D \to W_i W_j^* \to W_i \ell^+ \ell^-) \simeq \frac{\alpha \alpha_D \epsilon^2}{128\pi} m_{h_D} f_3(m_{W_i}/m_{h_D}), \tag{25}$$

where we have assumed $m_{W_i} = m_{W_j}$ for simplicity. This has the same form as the $h \to ZZ^*$ partial width in the standard model. The function $f_3(x)$, $\frac{1}{2} < x < 1$, is a 3-body phase space integral that can be found e.g. on page 30 in [45]. The decay length in the rest frame of h_D is shown in Fig. 11 for $\alpha_D = \alpha$ and for both $\epsilon = 10^{-5}$ and 10^{-8}. From the figure, we see that h_D decays can be prompt, displaced or invisible, depending on the parameters. Similarly diverse decay scenarios are also shown in Fig. 12, where we plot the h_D decay length after normalizing $\alpha_D \epsilon^2$ to its DAMA/LIBRA expected value.

If $m_{h_{D,\min}} < m_{W_{D,\min}}$, then the lightest Higgs can only decay through two off-shell gauge bosons, which is dominated by a four-fermion final state, and is parametrically given by

$$\Gamma(h_D \to W_D^* W_D^* \to 4\ell) \sim \frac{\alpha_D \alpha^2 \epsilon^4}{12\pi}. \tag{26}$$

A 2-body decay to two standard model fermions through a one-loop diagram mediated by W_D's is parametrically of the same size. Because of the strong ϵ^4 suppression, such a light Higgs is expected to escape the detector, even for large α_D. Note that in this case all but the very lightest Higgs have 3-body decays to either a lighter gauge boson or a lighter Higgs, so that it is not hard to construct dark sectors in which prompt, displaced, and invisible decays all occur.

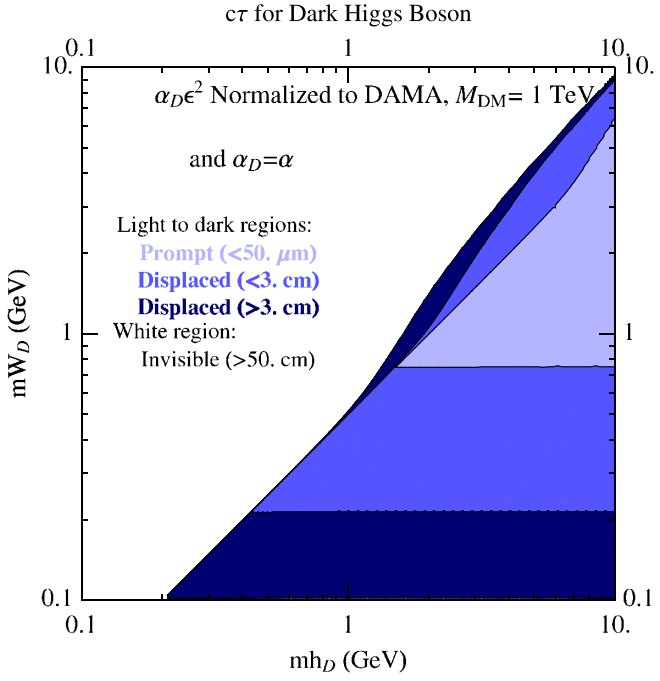

FIG. 12 (color online). Decay length ($c\tau$) of a dark-sector Higgs boson $h_D \to W_i W_j^* \to W_i \ell\ell$ as a function of its mass m_{h_D} and the dark-sector gauge boson mass m_{W_D}, for $\alpha_D = \alpha$. Here the combination $\alpha_D \epsilon^2$ has been normalized to its DAMA/LIBRA expected value, assuming that the dark matter (with mass 1 TeV) is part of the Higgsed dark sector and charged under the $U(1)_D$ (see Sec. II B for further explanation). The shaded regions in this figure are the same as in Fig. 11.

2. Event shapes in a Higgsed dark sector

Specific choices for the structure of a Higgsed dark sector can dramatically change the typical decay chains within the sector. It is typical for dark-sector production to result in a high-multiplicity and lepton-rich final state. Here, we discuss two examples.

A four-lepton final state is expected from production of a pair of metastable W_D bosons that decay directly to standard model fermions (Fig. 13(a)). The lepton kinematics depends on the W_D masses: if $m_{W_D} \ll \sqrt{s}$, then the observed leptons will lie in two approximately collinear pairs.

It is also possible to produce heavier gauge bosons that decay into a lighter W_D' and h_D of the dark sector, as in Fig. 13(b). One limit in which this is guaranteed is a dark sector with the structure of a charge-breaking standard model, with $SU(2)_D \times U(1)_D'$ Higgsed to $U(1)_D$ at m_{W_D} and with charge $(U(1)_D)$ being broken at a lower mass scale $m_{A'}$. Such models have an approximate global custodial symmetry $U(1)$ that suppresses the charged W_D's mixing with the A', so that the heavy W_D bosons are produced far more efficiently than the lighter A' [23]. In this case, a large number of leptons (and possibly pions) are expected. Likewise, it is possible to produce dark Higgs bosons directly (a special case is the "Higgs-strahlung" discussed in [16]).

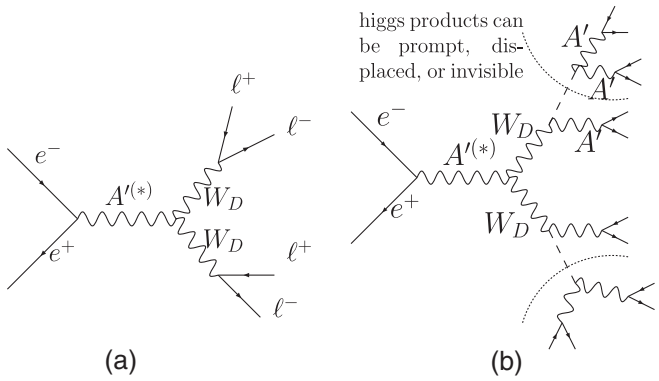

FIG. 13. Two examples of cascade decay chains for Higgsed dark sectors.(a) The production of a pair of dark-sector gauge bosons W_D can lead to a four-lepton event. (b) The production of a pair of heavy dark-sector gauge bosons, which decay within the dark-sector to lighter gauge and Higgs bosons, can lead to an event with a large number of leptons (and possibly pions).

3. Decay modes from additional mixing interactions

Additional couplings between the standard model and dark sector are possible, but they involve massive standard model-charged states and so are irrelevant to dark-sector production. They can, however, compete with the ϵ^4-suppressed decays of any light Higgs bosons in the dark sector. For example, the mixed Higgs quartic

$$\delta\mathcal{L} = \lambda_\epsilon |h_D|^2 |h_{\rm SM}|^2 \tag{27}$$

leads to Higgs decay through mixing with the standard model Higgs. If the theory is supersymmetric at high energies, $\lambda_\epsilon \sim \epsilon g g_D$ is generated by D-term mixing [23,46,47]. More generally, loops of link fields charged under G_D and $SU(2)_L \times U(1)_Y$ and loops of ordinary standard model matter will generate a quartic Higgs mixing through their Yukawa interactions with both Higgses. A rough upper bound on the mixing,

$$\lambda_\epsilon \lesssim \frac{m_{h_D}^2}{v_{\rm SM}^2}, \tag{28}$$

can be obtained by demanding that m_{h_D} receives at most $\mathcal{O}(1)$ corrections from this quartic term. If the $U(1)_D$ symmetry breaking is generated by (27), then this limit is saturated.

When h_D gets a vacuum expectation value, the quartic coupling (27) generates mixing between h_D and $h_{\rm SM}$ with angle

$$\theta \sim \frac{\lambda_\epsilon}{\lambda_{\rm SM}} \frac{v_D}{v_{\rm SM}} \to \frac{\lambda_\epsilon}{\lambda_{\rm SM}} \sqrt{\frac{\lambda_\epsilon}{\lambda_D}}, \tag{29}$$

where the latter limit corresponds to saturation of the bound (28). This mixing leads to a decay width

$$\Gamma(h_D \to \ell^+\ell^-)_{\rm mix} \sim \frac{y_\ell^2}{4\pi} m_{h_D} \theta^2 \to \frac{y_\ell^2}{4\pi} m_{h_D} \frac{\lambda_{\rm SM}}{\lambda_D} \left(\frac{m_{h_D}}{m_{h_{\rm SM}}}\right)^6, \tag{30}$$

where the final expression is again obtained by saturating (28). Assuming saturation, the decay length of h_D in its rest frame is given by

$$c\tau(h_D \to \ell^+\ell^-)_{\rm mix} \sim 7\ {\rm cm} \lambda_D \left(\frac{y_\ell}{y_\tau}\right)^{-2} \left(\frac{m_{h_D}}{3\ {\rm GeV}}\right)^{-7} \times \left(\frac{m_{h_{\rm SM}}}{120\ {\rm GeV}}\right)^4, \tag{31}$$

where $y_\tau \simeq 0.01$ is the τ Yukawa coupling. This decay can thus lead to observable decays with $\mathcal{O}$(cm) displacements if h_D is above the τ threshold, and saturates the naturalness bound. It dominates over the 3-body decay (25) if $\epsilon \lesssim 10^{-4}$. Below the τ threshold, however, it is unlikely to produce observable decays.

B. Events from a confined dark sector

In this section, we discuss the events obtained with confined dark sectors. We begin in Sec. III B 1 with a review of the spectroscopy in confined dark sectors containing one or multiple light flavors, and discuss the shape of production events. As for the Higgsed case, the events can usefully be characterized by discussing the metastable states, i.e. those states that do not decay to other dark-sector particles. For multiple light flavors, these metastable states are either the dark-sector pions (Sec. III B 2) or the A' (Sec. III B 3), depending on which is lighter. For a single flavor, the metastable states are either the A' (also Sec. III B 3), or the tower of mesons lighter than $2m_{\eta'_D}$, where $m_{\eta'_D}$ is the mass of the lightest meson (Sec. III B 4). Likewise, the lightest baryon Δ_D is exactly stable and a tower of baryons lighter than $m_{\Delta_D} + m_{\eta'_D}$ can be metastable.

1. Preliminaries: Spectroscopy and event shapes

We begin by reviewing the spectra of mesons and baryons in a one-flavor model. A model with only one light flavor has no light pion; instead, the lightest meson is expected to be a pseudoscalar meson ($J^{\rm PC} = 0^{-+}$), which we will call η'_D in analogy with the standard model η'. The second-lightest meson, again named by analogy with the standard model, is the ω_D (1^{--}). Excited states and higher-spin mesons are also expected, but their spectrum is not known precisely. We will only ever be interested in the tower of mesons with mass less than $2m_{\eta'_D}$. Mesons above this threshold can decay strongly to lighter mesons, and are quite broad. The one-flavor dark sector also contains a tower of baryons, beginning from the spin-$N_c/2$ Δ_D, where N_c is the number of colors of the confining gauge group. For small N_c, these have comparable mass to the tower of light mesons. We expect that any metastable glueball states will mix with the mesons, and decay through this mixing.

In a model with $N_f > 1$ light flavors, confinement breaks an approximate $SU(N_f)_L \times SU(N_f)_R \times U(1)$ flavor symmetry to a diagonal subgroup $SU(N_f)_d \times U(1)$. There are then $N_f^2 - 1$ light pions. All other mesons and (for $N_c > 2$) all baryons are parametrically heavier than the pions, and are produced much more rarely; therefore, we will focus on the pions.

The final-state kinematics and multiplicities can be estimated from those in the standard model by analogy with $e^+e^- \to$ hadrons processes and a simple rescaling of the QCD to dark-sector confining scale, or inferred from parametrizations such as the quark production rule [48]. These properties depend dominantly on the ratio of the confining scale to the energy $\sqrt{s_h}$ going into the confined sector ($\sqrt{s_h} = E_{\rm cm}$ for $e^+e^- \to$ hadrons or $e^+e^- \to$ dark-sector hadrons, while $\sqrt{s_h} = m_{A'}$ for the radiative return process). We will parametrize this by $R_E \equiv \sqrt{s_h}/m_{\eta'_D}$. Thus, for example, from low-energy SPEAR

data we see that jet structure is not observable for $R_E \approx 4$ (3.6 GeV collisions), but is observable by $R_E \approx 8$ [49].

Likewise, dark-hadron multiplicities can be estimated from QCD track multiplicities in e^+e^- collisions; what is measured is the charged-track multiplicities $\langle n_{\rm ch}\rangle$, not the total hadron multiplicity, but studies of the total energy of reconstructed tracks suggest that approximately half of produced hadrons are charged [49]. Doubling observed track multiplicities from e.g. [50,51], we see that over the range of interest, hadron multiplicities range between $\langle N\rangle \approx 10$ at 7.6 GeV ($R_E \approx 8$) to ≈ 40 at 90 GeV ($R_E \approx 100$).

At low R_E in a one-flavor model in which η'_D is the lightest state, we expect $\langle N\rangle \sim \sqrt{s}/m_{\eta'_D}$, so that the production of nonrelativistic hadrons dominates, while the production of a much lower multiplicity of hadrons is exponentially suppressed (see e.g. [52] for experimental evidence of this effect in QCD events with very few pions). It is difficult to make more quantitative statements in this region of parameter space based on either direct extrapolation from QCD or parametrized models. The QCD extrapolation would suggest hadron multiplicities larger than $E_{\rm cm}/m_{\eta'_D}$, which are consistent in theories with light pions but unphysical if the η'_D is the lightest state. Parametrizations such as the quark production rule [48] can in principle be modified for the one-flavor scenario, but they deviate from experimental data precisely at small R_E.

2. Dark sectors with metastable pions

In a model with two or more flavors and a heavy A', the lightest dark-sector states are pions. Since they are then kinematically forbidden to decay into any other dark-sector states, they are metastable.

Kinetic mixing does *not* generate the most general decays allowed for the dark pion in an effective field theory. In particular, the helicity-suppressed decay of a v-pion, $\pi_v \to \ell^+\ell^-$, which dominates in hidden valley models with a Z' that couples directly to *both* dark-sector and standard model matter, is not generated by kinetic mixing. This can be most readily seen before performing the field redefinitions that diagonalize the gauge field kinetic terms. Instead, let us treat the kinetic mixing as an insertion

$$\sim (g^{\mu\nu}p^2 - p^\mu p^\nu). \tag{32}$$

By Lorentz invariance, the pion current must have the form

$$\langle 0|A'_\mu|\pi(p)\rangle \propto ip_\mu, \tag{33}$$

which vanishes when dotted into the kinetic mixing tensor. In other words, kinetic mixing only mixes the transverse modes of the two gauge bosons, to which the pion does not couple. The vanishing of this decay mode is obscured when the couplings are diagonalized. The A' couples to the photon current $J_{\rm EM}$ but this vectorlike current vanishes

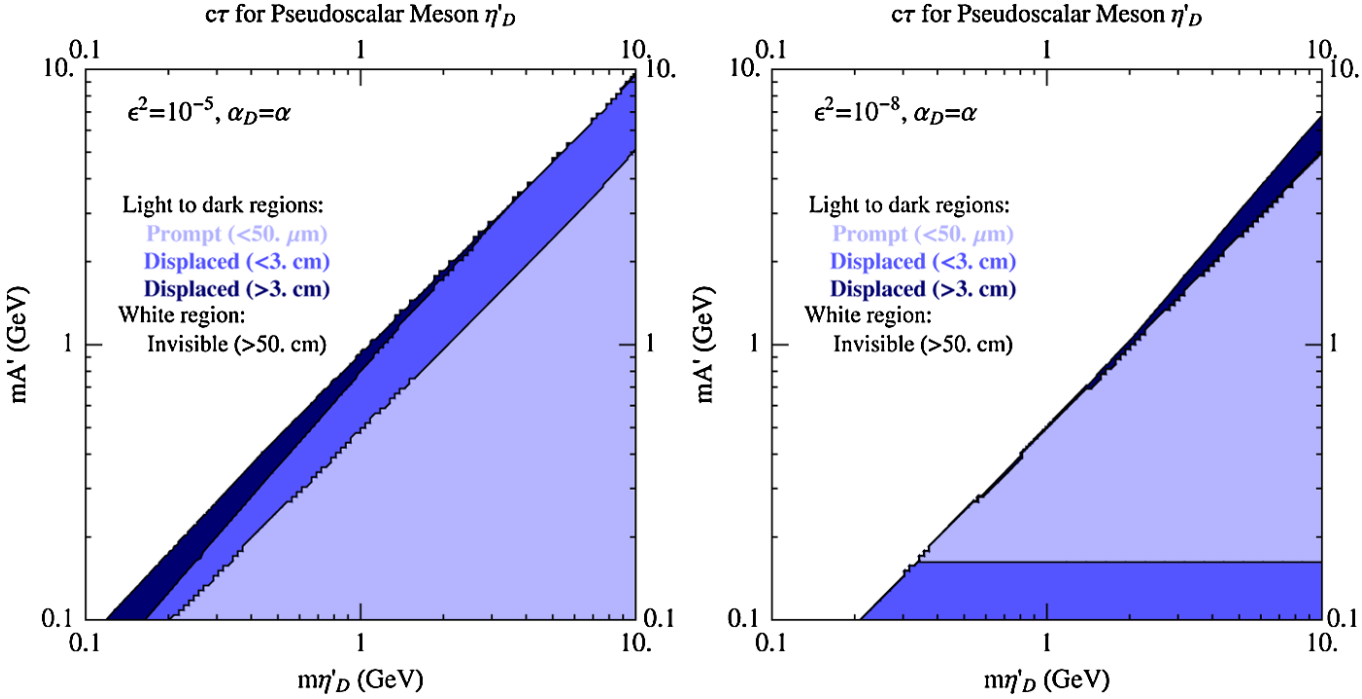

FIG. 14 (color online). Decay length ($c\tau$) of the dark-sector scalar meson η'_D, decaying through the axial anomaly to two on- or off-shell A' gauge bosons, which in turn decay into two standard model leptons or hadrons. Here $\alpha_D = \alpha$, and $\epsilon = 10^{-5}$ (left) or $\epsilon = 10^{-8}$ (right). The shaded regions in this figure are the same as in Fig. 11. This figure is also applicable to decays of light pions for dark sectors with multiple light flavors.

when contracted with p_μ. The A' also couples to the chiral current J_Z but this contribution is precisely canceled by the Z's coupling to the dark photon current $J_{A'}$, so this also does not mediate decays.

Instead, the pion can only decay through the anomaly diagram, but with one or both A' off-shell. The resulting decay width scales as

$$\Gamma_{\text{anomaly}}(\pi_D \to A'^{*} A'^{(*)}) \sim \frac{\alpha_D^2}{64\pi^3 f_{\pi_D}^2} m_{\pi_D}^3 \left(\frac{1}{4\pi}\alpha\epsilon^2 \frac{m_{\pi_D}^4}{m_{A'}^4}\right)^p, \tag{34}$$

where $p = 1$ for 3-body decays and $p = 2$ for 4-body decays, and the pion decay constant f_{π_D} can be estimated by scaling the pion decay constant in the standard model, $f_{\pi_D} = f_\pi m_{\eta'_D}/m_{\eta'_{\text{SM}}}$. These decay lifetimes are identical to those of the η'_D in a one-flavor model, and the rest frame displacements are shown in Fig. 14. If $m_{A'} < m_{\pi_D} < 2m_{A'}$, a 3-body decay can give rise to displaced vertices, but this mass condition is not generic. When $m_{A'} > m_{\pi_D}$, the 4-body mode is suppressed by ϵ^4, leading to very large displacements:

$$c\tau(\pi_D \to 4\ell) \sim \left(\frac{\alpha}{\alpha_D}\right)^2 \left(\frac{10^{-3}}{\epsilon}\right)^4 \left(\frac{1\ \text{GeV}}{m_{\pi_D}^3/f_{\pi_D}^2}\right) 10^{12}\ \text{cm}. \tag{35}$$

A loop decay to two leptons is also possible, but comparable in rate to the 4-body decay (in fact, it receives chiral suppression $\sim(m_\ell/m_{\pi_D})^2$ relative to the 4-body decay). Therefore, in this region of parameter space the pion escapes the detector without decaying, and is invisible.

Assuming that dark-sector interactions break the dark flavor symmetries, a heavier pion that cannot decay to two lighter pions may still decay via an off-shell A' into a lighter pion and standard model leptons/hadrons. This decay is suppressed by $\alpha_D\epsilon^2$, and so is typically prompt or displaced.

3. Dark sectors with a metastable light A'

In this section, we discuss the case when the A' is the lightest state in the dark sector. We consider both a one-flavor and a multiflavor model. In both cases, final states consisting of prompt standard model leptons and hadrons are likely.

A particularly simple example is the one-flavor model, in which the A' is significantly lighter than the dark mesons and the physical dark Higgs boson associated with $U(1)_D$ breaking, h_D. Under this assumption, the $\ell^+\ell^-\gamma$ production is important, but off-shell production of dark-sector particles gives rise to high-multiplicity final states consisting of leptons and/or standard model hadrons that may yield more sensitive limits.

For light A', all dark mesons and h_D can decay promptly to several A''s. For example, the η'_D decays through the chiral anomaly to $2A'$. We show the η'_D decay length in its rest frame in Fig. 14 for two different values of ϵ, and in Fig. 15 for the case that $\alpha_D\epsilon^2$ is normalized to its DAMA/LIBRA expected value. Heavier dark mesons may decay to two or more A''s, or to an A' and a lighter dark meson. Baryon number is an accidental low-energy symmetry of the dark sector, so we will assume that the Δ_D is exactly stable, and all other dark baryons decay to it and one or more A''s.

Therefore, all dark-sector final states eventually decay to a collection of A''s and stable Δ_D-baryons. The A' usually decays promptly through kinetic mixing [cf. Eqs. (22) and (23)]:

$$\Gamma(A' \to \ell^+\ell^-) = \frac{1}{3}\epsilon^2\alpha m_{A'}\sqrt{1-\frac{4m_\ell^2}{m_{A'}^2}}\left(1+\frac{2m_\ell^2}{m_{A'}^2}\right)N_{\text{eff}}$$

$$\Rightarrow c\tau(A' \to \ell^+\ell^-) \sim 8\times 10^{-6}\ \text{cm}\left(\frac{10^{-3}}{\epsilon}\right)^2\left(\frac{1\ \text{GeV}}{m_{A'}}\right)\left(\frac{1}{N_{\text{eff}}}\right). \tag{36}$$

We expect to produce final states with at least one to two A'

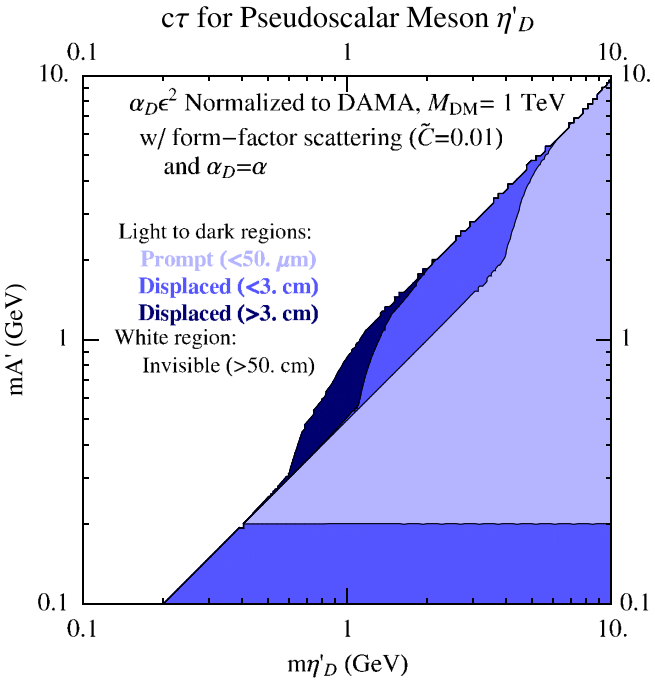

FIG. 15 (color online). Decay length ($c\tau$) of the dark-sector scalar meson η'_D, decaying through the axial anomaly to two on- or off-shell A' gauge bosons, which in turn decay into two standard model leptons or hadrons. Here $\alpha_D = \alpha$, and the combination $\alpha_D\epsilon^2$ has been normalized to its DAMA/LIBRA expected value, assuming that the dark matter is a 1 TeV dark meson neutral under $U(1)_D$, but consists of a light and a heavy quark charged under $U(1)_D$ (see Sec. II B). The shaded regions in this figure are the same as in Fig. 11. This figure is also applicable to decays of light pions for dark sectors with multiple light flavors.

per dark hadron. These decays can easily generate high lepton multiplicities, even when relatively few dark hadrons are produced.

In one-flavor models at high multiplicities, production of dark baryons is unavoidable and leads to invisible products which escape the detector. For low-multiplicity final states, when $\sqrt{s}/m_{\eta'} \sim 2$, the efficiency for producing individual exclusive final states, such as those that do not contain any baryons, are reasonably high.

Similar comments apply for multiflavor models, in which the pions are significantly heavier than the A'. In this case, some pions may be stabilized by unbroken dark-sector flavor symmetries, or by an unbroken discrete subgroup of $U(1)_D$ if their charges are noninteger multiples of the dark Higgs charge. Kinetic mixing does not change the stability of these pions, and they will escape the detector. Pions that are not stabilized, however, can decay to $2A'$ through the chiral anomaly, and these A''s are observable through their prompt decays to standard model matter.

4. Dark sectors with towers of metastable mesons and baryons

We now consider the one-flavor model with a heavy A'. If the A' is heavy, then the tower of mesons lighter than $2m_{\eta'_D}$ becomes metastable, i.e. they have no available decays within the dark sector. These decays are therefore suppressed by at least ϵ^2, and can often be displaced or even invisible. Likewise, all baryons lighter than $m_{\Delta_D} + m_{\eta'_D}$ are metastable for heavy A'.

The discussion of dark pion decays in Sec. III B 2 applies to the η'_D as well. In particular, decays must proceed through *two* A' gauge bosons, and if both are off-shell they are suppressed by ϵ^4. Therefore, they can easily be invisible. The decay of η'_D through one or two off-shell A''s is included in Figs. 14 and 15.

The decays of the heavier mesons are generically much easier to see. The ω_D vector meson generically mixes with the A', with a mixing angle that can be estimated from their masses,

$$\theta \sim \frac{m_{\omega_D}^4}{(m_{\omega_D}^2 + m_{A'}^2)^2}. \tag{37}$$

This leads to a decay width that is suppressed by ϵ^2, and up to an unknown $\mathcal{O}(1)$ coefficient is given by

$$\Gamma(\omega_D \to \ell^+\ell^-) \sim \frac{4\pi}{3}\epsilon^2\alpha\alpha_D \frac{m_{\omega_D}^5}{(m_{\omega_D}^2 + m_{A'}^2)^2} \times \sqrt{1 - \frac{4m_\ell^2}{m_{\omega_D}^2}}\left(1 + \frac{2m_\ell^2}{m_{\omega_D}^2}\right). \tag{38}$$

The total ω_D width depends only mildly on m_{ω_D}. In Fig. 16, we show $c\tau$ for ω_D for two different values of ϵ, while in Fig. 17, we normalize $\alpha_D\epsilon^2$ to its DAMA/LIBRA expected value.

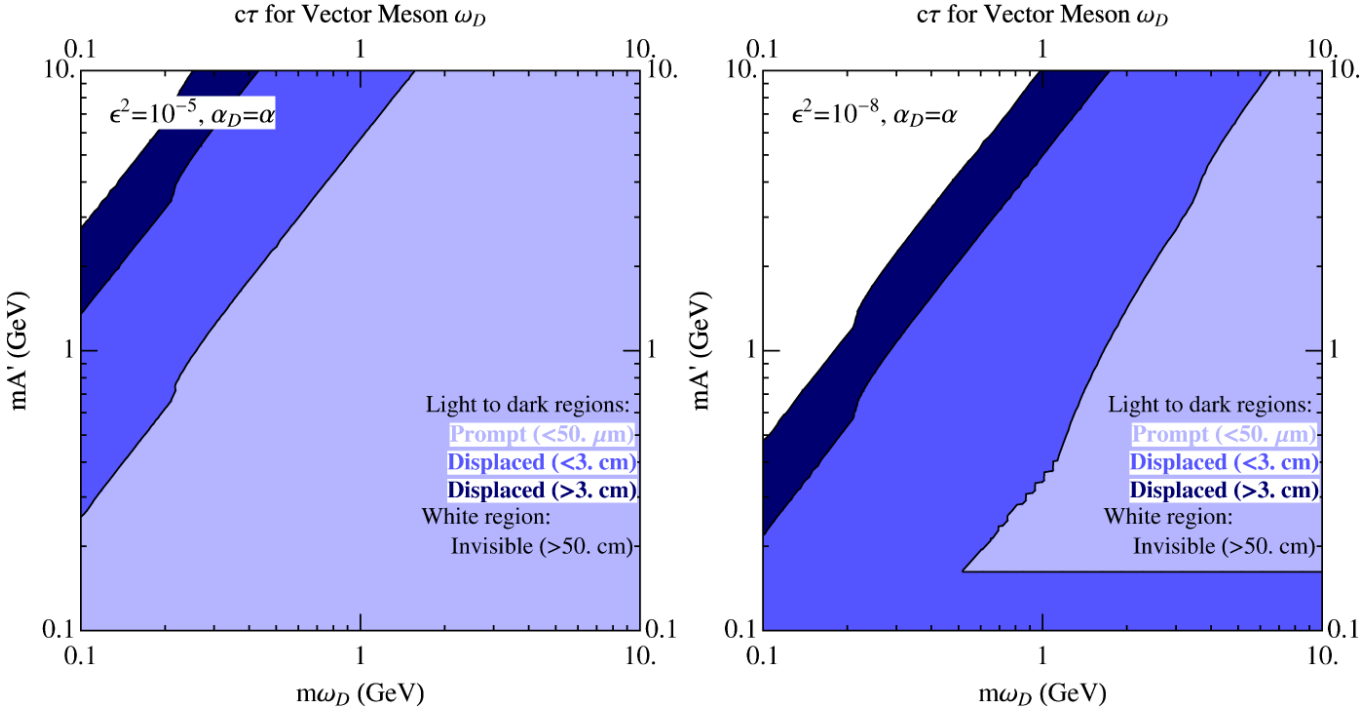

FIG. 16 (color online). Decay length ($c\tau$) of the dark-sector vector meson ω_D, which mixes with the A' and decays to two standard model leptons or hadrons. Here $\alpha_D = \alpha$, and $\epsilon = 10^{-5}$ (left) or $\epsilon = 10^{-8}$ (right). The shaded regions in this figure are the same as in Fig. 11.

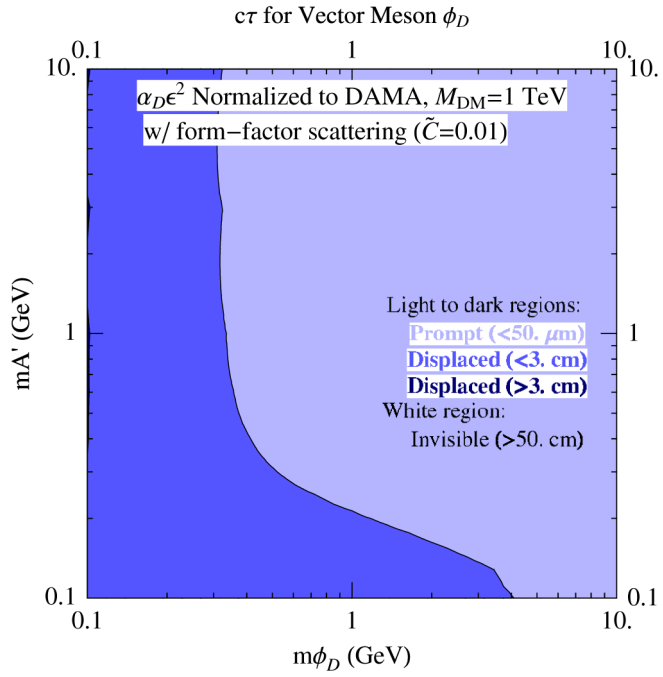

FIG. 17 (color online). Decay length ($c\tau$) of the dark-sector vector meson ω_D, which mixes with the A' and decays to two standard model leptons or hadrons. Here $\alpha_D = \alpha$, and the combination $\alpha_D\epsilon^2$ has been normalized to its DAMA/LIBRA expected value, assuming that the dark matter is a 1 TeV dark meson neutral under $U(1)_D$, but consists of a light and a heavy quark charged under $U(1)_D$ (see Sec. II B). The shaded regions in this figure are the same as in Fig. 11.

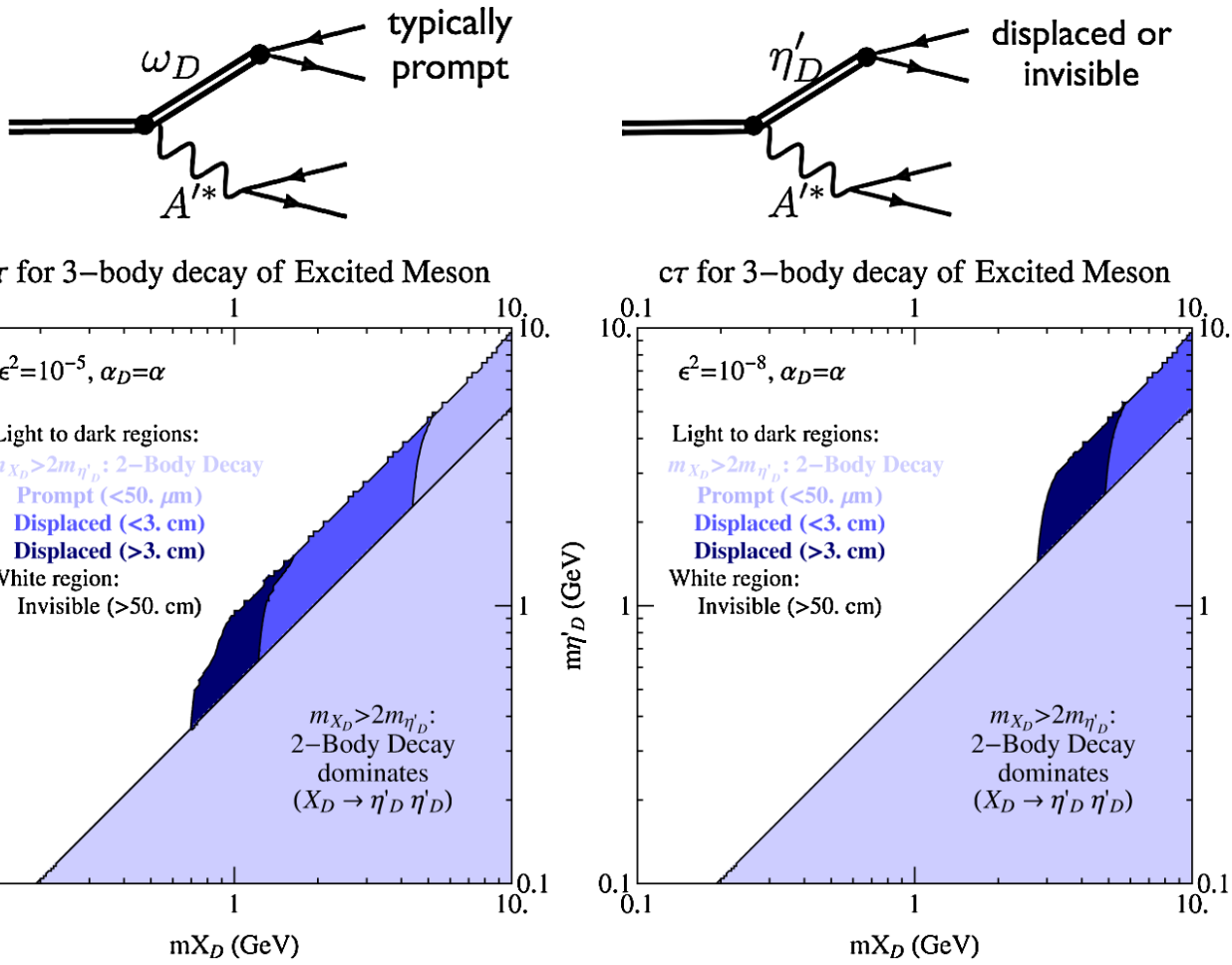

FIG. 18 (color online). Top: Diagram showing 3-body decays of a heavy dark-sector excited spin-0 and spin-2 meson X_D into standard model states (through an off-shell A') and a lighter meson. Bottom: Decay length ($c\tau$) of X_D. Here $\alpha_D = \alpha$, and $\epsilon = 10^{-5}$ (left) or $\epsilon = 10^{-8}$ (right). In the very light blue region (lower right triangle) the 2-body decay of X_D dominates. The remaining shaded regions in this figure are the same as in Fig. 11.

Exotic and excited mesons can have more spectacular decays. Spin-1 mesons are expected to decay into standard model pairs, just like the ω_D, while spin-0 and spin-2 mesons can have 3-body decays into standard model states (through an off-shell A') and a lighter meson, as shown in Fig. 18. These have a typical lifetime, estimated by dimensional analysis, given by

$$\Gamma(X_D \to A'^* + (\omega_D/\eta'_D) \to \ell^+\ell^- + (\omega_D/\eta'_D)) \sim \frac{\alpha_D \alpha \epsilon^2}{12\pi} \frac{m_{X_D}^5}{m_{A'}^4} \sqrt{1 - \frac{m_{\omega_D/\eta'_D}^2}{m_{X_D}^2}}, \quad (39)$$

which can easily be displaced. This is shown in Fig. 18 for two different values of ϵ, and in Fig. 19 for a case in which $\alpha_D\epsilon^2$ has been normalized to its DAMA/LIBRA expected value.

Note that, unlike the decay of the η'_D into standard model states, where the 3-body region of phase space required a tuning of independent masses $m_{\eta'_D}$ and $m_{A'}$, the condition $m_{\eta'_D/\omega_D} < m_{X_D} < 2m_{\eta'_D}$ is satisfied naturally for a tower of exotic mesons X_D. Similar decays are expected for excited baryons.

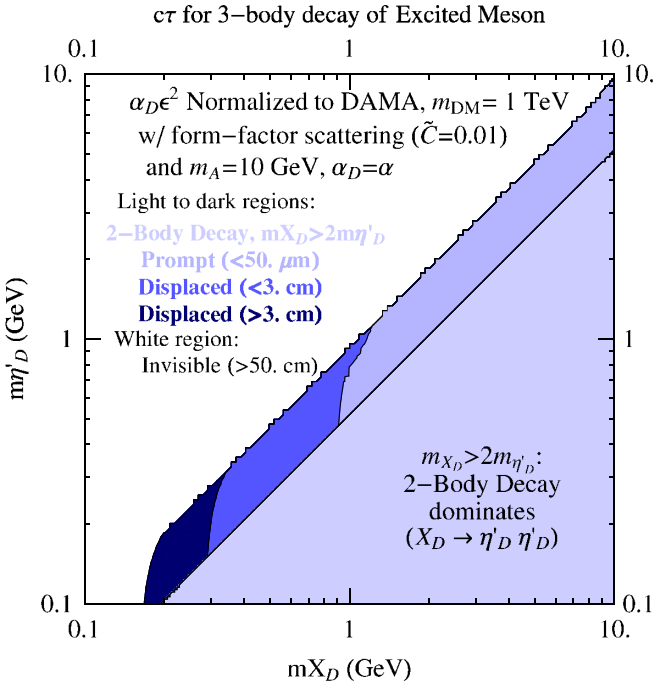

FIG. 19 (color online). Decay length ($c\tau$) of a heavy dark-sector spin-0 and spin-2 excited meson X_D, which has a 3-body decay to a lighter meson and to two standard model leptons or hadrons through an off-shell A'. Here $\alpha_D = \alpha$, and the combination $\alpha_D\epsilon^2$ has been normalized to its DAMA/LIBRA expected value, assuming that the dark matter is a 1 TeV dark meson neutral under $U(1)_D$, but consists of a light and a heavy quark charged under $U(1)_D$ (see Sec. II B). In the very light blue region (lower right triangle) the 2-body decay of X_D dominates. The remaining shaded regions in this figure are the same as in Fig. 11.

To summarize: although significant missing energy from both baryons and η'_D's is generically expected, typical events in such a sector *also* have a combination of prompt and displaced decays.

C. Dark sectors with uncolored fermions

We have focused on Higgsed and confined sectors with no light fermions. However, the presence of a light fermion changes the phenomenology of either a Higgsed or a confined dark sector dramatically. Some or all of the bosons that are produced can decay to two dark-sector fermions, instead of decaying to standard model fermions through kinetic mixing. The dark-sector fermions are singlets under any confining gauge group (in the confined case, the dark-sector gauge group may have a subgroup which does not confine). The lightest dark-sector fermion does not have any decay modes induced by kinetic mixing, but can decay through new mixing operators of the form

$$\frac{c}{M^p}(L_D h_D^p)(L h_{\rm SM}), \quad (40)$$

where h_D^p is a collection of dark-sector Higgses with the same quantum numbers as a dark-sector fermion L_D, L is a standard model fermion, and $h_{\rm SM}$ is a standard model Higgs. The decay lifetime of the dark fermions is quite model-dependent, but they will typically be long-lived. In this case, any dark-sector bosons that can decay to a pair of light dark-sector fermions may well be invisible. The only way to find such invisible sectors is by observing their recoil against other particles in the final state (in the context of B-factories, a photon).

In dark sectors with more than one light fermion, this situation is ameliorated. The second-lightest fermion f_2 may have decays, through either Higgs quartic or gauge boson kinetic mixing,

$$f_2 \to f_1 A' \to f_1 \ell^+\ell^-, \quad (41)$$

where the A' may be on- or off-shell. This decay is especially important when the decay $f_2 \to 3f_1$ is kinematically not allowed. These fermions generically have longer decay lifetimes than their bosonic counterparts by the ratio of 3-body to 2-body phase space $\sim 1/16\pi^2$. Such decays are much harder to find than the bosonic analogues because they contain missing energy, and the $\ell^+\ell^-$ invariant mass need not reconstruct a resonance. Instead, the dilepton invariant mass distribution may have an end point. Moreover, if a sector contains both metastable fermions *and* metastable bosons, the bosonic decay products may reconstruct resonances.

IV. SEARCHES AT LOW-ENERGY e^+e^- COLLIDERS

Experiments at high-intensity e^+e^- colliders at low energies, such as the B-factories *BABAR* and BELLE, can open a direct window into the physics of a low-mass dark sector by observing production of dark-sector particles and their decays back into the standard model. Though striking, these final states are quite different from those of interest for precision measurements of the standard model, and could have gone unnoticed in existing B-factory data sets. A common feature of the dark-sector production processes is a high-multiplicity of leptons, pairs of which reconstruct resonances. However, the precise multiplicity and energy of these leptons, and the presence of displaced vertices or missing energy, depend on the detailed structure of the dark sector.

This variety makes inclusive searches desirable, but the primary concern is maintaining acceptance for a large fraction of signal events while removing standard model backgrounds. To this end, we identify several search strategies, with exclusive search requirements for events with large physics backgrounds and inclusive treatments for more striking signal events. Our discussion is mostly qualitative; a quantitative study is beyond the scope of this paper. Our focus is on *BABAR* and BELLE, which represent the current high-intensity frontier, but similar analyses with data from KLOE, CLEO-c, the upcoming BES-III [53], and elsewhere could be more sensitive, depending on the nature of the dark sector.

We identify six regions of interest, where different search strategies are required:

(1) 4ℓ (exclusive), reconstructing $E_{\rm cm}$ (also $4\ell + \gamma$)
(2) 4ℓ (exclusive), with displaced dilepton vertices (also $4\ell + \gamma$)
(3) $\geq 5\ell$ + tracks (inclusive), reconstructing $E_{\rm cm}$ (also + γ)
(4) $\geq 5\ell$ + tracks (inclusive), with displaced dilepton vertices (also + γ)
(5) Very high track multiplicity, with many tracks consistent with leptons
(6) γ + nothing

Before discussing each of these searches in turn, we list three prominent physics backgrounds that contribute to the channels with four or more leptons:

(1) QED processes, $e^+e^- \to 4\ell$, which can reconstruct the full beam energy.
(2) Two photons, emitted from the initial-state electron and positron, can combine to produce e^+e^-, $\mu^+\mu^-$, or $\pi^+\pi^-$ pairs. The electron and positron are usually, but not always, lost along the beam pipe. A four-lepton event is obtained if the initial state pair is observed, or if an additional γ^* produces two more leptons. The latter kind of event can be rejected by requiring reconstruction of the full beam energy.
(3) Sequential leptonic B decays produce events with up to four leptons, plus additional tracks; some energy is carried by neutrinos so these events do not reconstruct the full beam energy.

4ℓ *exclusive*, *reconstructing* $E_{\rm cm}$ (*with or without* γ).—Four-lepton final states ($\mu^+\mu^-\mu^+\mu^-$, $\mu^+\mu^-e^+e^-$, and $e^+e^-e^+e^-$) that reconstruct the full beam energy can be produced by the simplest decay chains in Higgsed sectors (Fig. 13(a)), or by confined sectors with $m_{\eta'_D} \lesssim E_{\rm cm}/4$. These processes also produce τ and hadronic final states, but these are harder to search for, whereas muons have the lowest backgrounds. Requiring the reconstruction of the full beam energy $E_{\rm cm}$ removes the physics backgrounds (2) and (3) mentioned above, but also makes these searches insensitive to production modes that include stable or long-lived final states, such as baryons or metastable Higgs bosons. Pairs of leptons should reconstruct very narrow (resolution-limited) resonances, which can be used as a very useful discriminator between signal and background. The two lepton pairs need not reconstruct the same mass, but it is likely that they will reconstruct indistinguishable masses in an $\mathcal{O}(1)$ fraction of events. Similarly, $4\ell + \gamma$ final states can be produced by simple Higgsed-sector decays, or by confined sectors with $m_{\eta'_D} \lesssim m_{A'}/4$ and $m_{A'} < E_{\rm cm}$. In this case, in addition to pairwise mass reconstruction as in the pure 4ℓ case, the four leptons should now also reconstruct a (potentially broader) A' resonance.

4ℓ *exclusive with displaced vertices* (*with or without* γ).—The requirement of displaced vertices allows significant reduction of standard model backgrounds (1) and (2), without demanding that the observed products reconstruct the full beam energy $E_{\rm cm}$. In an exclusive four-lepton final state, background (3) is also negligible. Dropping the $E_{\rm cm}$ requirement is quite important—in scenarios with displaced vertices, it is also generic to have missing energy coming from long-lived particles decaying outside the detector, or exactly stable baryons. For example, a confined sector with one light flavor can have displaced ω_D decays, and long-lived invisible η'_D decays. Similarly, the beam-energy requirement can be relaxed in a $4\ell + \gamma$ search and replaced by a displaced vertex cut. In this case, a four-lepton reconstructed mass peak is *no longer* expected as some of the A' mass can go into invisible decays. Pairs of same-flavor leptons should still reconstruct narrow resonances.

$\geq 5\ell$ *exclusive* (*with* $E_{\rm cm}$ *or displaced vertices, with or without* γ).—More complex Higgsed-sector decay chains such as Fig. 13(a), where the Higgs decays within the detector, or confined-sector decays with larger ratio $E_{\rm cm}/\Lambda_D$ can generate moderate track multiplicities. We stress that, though the leptonic final states are most distinctive, especially at higher masses the dark resonances *will* decay to τ and hadronic states as well. Therefore, it is essential not to veto on nonleptonic tracks, and to tag

leptons as loosely as possible to suppress backgrounds. It may also be interesting to specifically search for events with $\tau^+\tau^-$ or $\pi^+\pi^-$ pairs. Therefore, a more inclusive approach is warranted, i.e. requiring five or six leptons to reduce background, plus additional tracks. As in the 4ℓ searches, two complementary cuts are useful for discriminating from background: either full reconstruction of $E_{\rm cm}$ or displaced vertices.

High track multiplicities.—A confined dark sector with $m_{\eta'_D} \sim m_{\eta'_{\rm QCD}}$ produces a high multiplicity $\sim$10–20 dark hadrons, of which a significant fraction decays visibly within the detector. The resulting dark-sector parton shower can lead to somewhat collimated jets of decay products. A large fraction (between $4/5$ and $1/3$ depending on meson mass) of dark mesons go into e or μ pairs, and this can be used to assist in distinguishing these final states from backgrounds. There is no source of analogous events from a Higgsed dark sector without a confined group.

γ + nothing.—A further interesting region of parameter space is when all the produced dark-sector states decay outside the detector, in which case all dark-sector products are invisible. This occurs, for example, if all states in the dark sector can decay to a long-lived pion or dark Higgs. In this case, the γ + nothing mode is the only effective search at low-energy e^+e^- colliders (see also [17]). These events can be detected by observing a peak in the photon energy spectrum at $\sqrt{s} \simeq m_{A'}$.

The searches mentioned above are complementary to the dilepton resonance searches ($e^+e^- \to \gamma A' \to \gamma\ell^+\ell^-$) that have recently been discussed in [17,36,41]. However, the $A' \to \ell^+\ell^-$ decay is significant only when the A' is the lightest state in the dark sector. Even if the A' is the lightest state of the dark sector, any other kinematically accessible states are pair-produced with a comparable rate through an off-shell A', which produces a signal in the multilepton channel, which has much lower QED backgrounds. The multilepton searches considered here overlap with the four- and six-lepton searches discussed in [16] in the context of Abelian dark sectors, but we emphasize that much higher multiplicities are easily obtained in more general non-Abelian dark sectors.

V. CONCLUSIONS

Evidence for a low-mass dark sector may be hidden in unexamined e^+e^- collider data. If the new sector contains a $U(1)_D$ factor, then moderately large kinetic mixing $\epsilon \sim 10^{-3}$ is not only generated by generic mechanisms, but suggested by a variety of experiments and observations that look for dark matter. States of a new sector with couplings in this range can be efficiently produced in e^+e^- colliders, and may decay spectacularly, so that potential discoveries are within the reach of searches in existing data from low-energy e^+e^- collider experiments such as *BABAR*, BELLE, CLEO-c, and KLOE.

The evidence for a "dark sector" from terrestrial and satellite searches for dark matter is indirect, but strikingly consistent. The large local electron/positron excesses reported by HEAT, PAMELA, PPB-BETS, and ATIC suggest interactions of $\mathcal{O}$(TeV)-mass dark matter with a new boson with mass $\mathcal{O}$(1 GeV). Simultaneously, two experiments suggest multiple dark matter states with small mass splittings: the INTEGRAL 511 keV-line and DAMA/LIBRA modulation signal are consistent with 1–10 MeV and $\sim$100 keV splittings among dark matter states, respectively. New forces, Higgsed or confined at $\mathcal{O}$(GeV), can give rise to these splittings. Any subset of these results suggests a departure from the standard minimal WIMP paradigm, but dark matter data will provide at best an indirect probe of such structure.

If the DAMA/LIBRA modulation signal comes from inelastic scattering mediated by kinetic mixing, then it is the first quantitative probe of kinetic mixing between the standard model and the dark sector, and can be used to estimate the production rate of new dark-sector particles. If the mass of the new $U(1)_D$ gauge boson is $m_{A'} \simeq 1$ GeV, cross sections $\simeq 0.1$ fb are expected in a Higgsed dark sector with $\alpha_D \simeq \alpha$. This estimate leads to 50–100 events expected in the stored data sets from *BABAR* and BELLE. The e^+e^- production cross section normalized to DAMA/LIBRA scales as $m_{A'}^4$, so much larger cross sections ($\mathcal{O}$(pb)) are possible for a heavier A', while higher-luminosity experiments are required to observe dark sectors with lower $m_{A'} \sim$ 100's of MeV. Cross sections up to 100 fb are possible even for a 1 GeV A', if the DAMA/LIBRA scattering is suppressed by a form factor, as expected in confined models.

Though spectacular, the signatures of dark-sector production at e^+e^- colliders would still have been missed by existing searches. The precise final states depend on the spectroscopy of the dark sector—general regions of parameter space allow a combination of prompt and displaced decays, as well as states that escape the detector invisibly before decaying. All decay modes are expected to produce lepton-rich final states. Moderate multiplicities (4–10) of leptons and very high multiplicities are both possible, and require different search strategies. Some of these lepton pairs are expected to reconstruct very narrow resonances, which in principle can be combined to reconstruct the spectrum of the dark sector. Dark sectors with very long-lived final states may only be visible in a γ + nothing search. Further work to optimize the strategies proposed here and study their efficiencies is an important task.

The small production cross sections for $m_{A'} \lesssim 100$ MeV pose a particular challenge. Novel experiments are called for to explore this region. Two features of the low-mass region are noteworthy. Lower-energy $\mathcal{O}$(100 MeV) colliders may reach higher luminosities than can be attained at GeV-energy colliders. Moreover, not far below the cross

section reach of B-factories, at $\epsilon \sim 10^{-6}$, the expected decay lengths of spin-1 states in the dark sector become $\mathcal{O}(1\text{ m})$, so that very different techniques, such as beam-dump experiments, may be the most fruitful way to isolate dark-sector production events.

Dark matter experiments suggest new low-energy gauge interactions beyond the standard model. If a dark sector exists, it dramatically reshapes our understanding of the structure of nature. Searches in existing collider data offer a simple but powerful probe of this new dynamics and should be pursued.

ACKNOWLEDGMENTS

We are grateful to Daniele Alves, Nima Arkani-Hamed, Siavosh Behbahani, Howard Haber, Jay Wacker, and Neal Weiner for many fruitful discussions. We especially thank Mathew Graham and Aaron Roodman for numerous discussions regarding *BABAR* physics, and Michael Peskin for helpful feedback on our analysis of production and decay phenomenology. R. E. and P. C. S. are supported by the US DOE under Contract No. DE-AC02-76SF00515.

APPENDIX A: CONSTRAINTS ON KINETIC MIXING BETWEEN HYPERCHARGE AND A NEW $U(1)_D$

In this appendix, we review the most important existing constraints on the kinetic mixing between standard model hypercharge and $U(1)_D$.

For low-mass (MeV–GeV) dark photons A', there are a variety of constraints on the kinetic mixing that are summarized in [36] (for a discussion of searches for even lower mass dark photons see [54,55]). Constraints from big-bang nucleosynthesis disfavor $m_{A'} \lesssim \mathcal{O}$ (few MeV) [56]. For $m_{A'} \lesssim 10$ MeV, the strongest constraints come from the A' contribution to the anomalous magnetic moment of the electron $a_e^{A'}$, while for $m_{A'}$ above 10 MeV, but less than a few GeV, the tightest constraints come from the A' contribution to the anomalous magnetic moment of the muon $a_\mu^{A'}$. For $m_{A'} \sim \mathcal{O}(100\text{ MeV–}300\text{ MeV})$, constraints from certain rare decays of mesons, such as $K^+ \to \pi^+ A'$, are in some cases competitive with the constraint on $a_\mu^{A'}$, but depend sensitively on the decay modes of the A'—see [36] for a more detailed discussion. Above a few GeV, kinetic mixing is only very weakly constrained. However, since kinetic mixing also induces a coupling between the Z and dark-sector matter, a potential probe could come from searches for rare Z-decays.

Since we are interested in the mass range $m_{A'} \sim$ 10 MeV–20 GeV, we focus on the constraint on $a_\mu^{A'}$ and the potential probe coming from rare Z-decays.

Anomalous lepton magnetic moments.—Let us first discuss the contribution from the A' to the anomalous magnetic moment of a lepton ℓ. This was calculated in [36], and is given by

$$a_\ell^{A'} = \frac{\alpha\epsilon^2}{2\pi}\int_0^1 dz \frac{2m_\ell^2 z(1-z)^2}{m_\ell^2(1-z)^2 + m_{A'}^2 z}. \tag{A1}$$

For $a_e^{A'}$, this can be converted to a constraint of $\epsilon^2 \lesssim 10^{-5}(m_{A'}/(10\text{ MeV}))^2$ [36], which is important for $m_{A'} \lesssim 10$ MeV. A constraint on $a_\mu^{A'}$ is more ambiguous, since the theoretical prediction for the muon anomalous magnetic moment within the standard model a_μ involves a hadronic contribution which must be estimated from experiments, which do not all agree. Using data from e^+e^- annihilation to hadrons, the theoretical value of a_μ is smaller than the measured value by $(302 \pm 88) \times 10^{-11}$, a 3.4σ deficit [37,38]. However, estimates involving data from τ's [57] or from preliminary *BABAR* results on the precision measurement of the $e^+e^- \to \pi^+\pi^-(\gamma)$ cross section with the initial state radiation method [58] do not point to a significant discrepancy. Since the A' contribution to a_μ is positive, a conservative constraint on the $\epsilon - m_{A'}$ parameter space is obtained by taking the estimate from e^+e^- annihilation to hadrons. In particular, for the constraints shown in Sec. II, we follow [36] and require $a_\mu^{A'} < (302 + 5\sigma) \times 10^{-11} = 7.4 \times 10^{-9}$. For $m_{A'} \gg m_\mu$, Eq. (A1) reduces to $a_\mu^{A'} \simeq \frac{\alpha\epsilon^2 m_\mu^2}{3\pi m_{A'}^2}$, and the constraint on $a_\mu^{A'}$ thus becomes very weak for $m_{A'}$ larger than a few GeV.

Exotic Z decays.—For $m_{A'}$ larger than m_μ, searches for exotic Z-decays among the 2×10^7 Z-bosons recorded by the experiments at LEPI could potentially probe kinetic mixings more sensitively than a_μ. Let us discuss this in more detail. The coupling induced between the Z and dark-sector fermions is given by

$$\mathcal{L} \supset -\sum_{i=1}^{N_f} \epsilon g_D \tan\theta_W Z_\mu \bar{X}\gamma^\mu X, \tag{A2}$$

where N_f is the number of dark-sector particles coupling to A' with gauge coupling g_D, and $\sin\theta_W$ is the standard model weak-mixing angle. In this expression, the A' coupling to the electromagnetic current has been normalized as $\mathcal{L} \supset \epsilon g_D A'_\mu J^\mu_{\text{EM}}$ [see Eq. (1)]. The Z-decay width to dark-sector fermions is thus

$$\Gamma(Z \to \bar{X}X) \sim \frac{1}{3} N_c \epsilon^2 \alpha_D m_Z \tan^2\theta_W \times \sum_{i=1}^{N_f} \sqrt{1 - \frac{4m_X^2}{m_Z^2}}\left(1 + \frac{2m_X^2}{m_Z^2}\right), \tag{A3}$$

where N_c is the number of colors of the dark-sector gauge group.

Since the total width of the Z has been measured to be 2.4952 ± 0.0023 GeV [39], the branching ratio of $Z \to \bar{X}X$ is given by

$$\text{BR}(Z \to \bar{X}X) \sim 2.8 \times 10^{-8} N_c \frac{\alpha_D}{\alpha}\left(\frac{\epsilon}{10^{-3}}\right)^2, \tag{A4}$$

where we assumed $m_X \ll m_Z$. Depending on the decay modes of X, which we discussed in detail in Sec. III, a variety of signatures is possible. For example, if the X's decay invisibly or outside the detector, the constraint is not better than the uncertainty on the width of the Z, which is about 0.1%. More exotic Z-decays into multileptons are possible, but require dedicated searches. The best constraints on rare Z-decay branching ratios are no better than the 10^{-6}–10^{-5} level [39], and even dedicated searches may not reach this level for complicated final states. Equation (A4) shows that for typical parameters that give $\mathcal{O}$(fb) cross sections at B-factories, the branching ratio $Z \to \bar{X}X$ is about 3 orders of magnitude smaller than what could be probed at LEPI even with a dedicated search. For the multilepton final states we consider in this paper, the B-factories will thus be a far more sensitive probe of the $\epsilon - m_{A'}$ parameter space than LEPI, at least for $m_{A'}$ less than a few tens of GeV.

APPENDIX B: DAMA/LIBRA NORMALIZATION OF COUPLINGS

Inelastic dark matter offers a simple explanation that reconciles the annual modulation signal reported by DAMA/LIBRA with the null results of other experiments, and is reviewed in [12,13]. Below, we summarize our procedure for normalizing $\alpha_D\epsilon^2$ assuming that DAMA/LIBRA is explained by an iDM mechanism. We will normalize $\alpha_D\epsilon^2$ for two iDM scenarios: one in which the inelastic channel proceeds through charged-current scattering as in [12], and one where the inelastic channel is through a hyperfine transition as in [9].

For charged-current scenarios, the inelastic cross section to scatter off of a nucleus of mass m_N and charge Z recoiling with energy E_R is

$$\frac{d\sigma}{dE_R} \approx \frac{8\pi Z^2 \alpha \alpha_D \epsilon^2 m_N}{v^2} \frac{1}{(2m_N E_R + m_{A'}^2)^2} |F(E_R)|^2, \tag{B1}$$

where α is the fine structure constant, v is the dark matter-nucleus relative velocity, and $m_{A'}$ is the A' mass. $F(E_R)$ is the Helm nuclear form factor [59], and it accounts for the loss of coherence scattering off of the entire nucleus at large recoil. We use

$$|F(E_R)|^2 = \left(\frac{3j_1(|q|r_0)}{|q|r_0}\right)^2 e^{-s^2|q|^2}, \tag{B2}$$

where $s = 1$ fm, $r_0 = \sqrt{r^2 - 5s^2}$, $r = 1.2A^{1/3}$ fm, and $|q| = \sqrt{2m_N E_R}$.

For hyperfine transition scattering [9], the inelastic cross section is

$$\frac{d\sigma}{dE_R} \approx \frac{4\pi Z^2 \alpha c_{\rm in}^2 \alpha_D \epsilon^2}{v^2 \Lambda_D^2} \frac{m_N^2 E_R}{(2m_N E_R + m_{A'}^2)^2} |F(E_R)|^2, \tag{B3}$$

where $c_{\rm in}/\Lambda_D \sim \text{GeV}^{-1}$ is the A' electric dipole of the dark matter. To fix the relation between Λ_D and the hyperfine splitting δ in this case, we introduce a scale $\tilde{\Lambda}_D$ such that

$$\delta = \frac{\tilde{\Lambda}_D^2}{m_{\rm DM}}. \tag{B4}$$

As discussed in Sec. II B, $\tilde{\Lambda}_D/\Lambda_D$ is naturally a small number. We will therefore normalize $\alpha_D\epsilon^2$ as a function of $m_{A'}$ for different choices of the small dimensionless coefficient,

$$\tilde{C} = \left(\frac{c_{\rm in}^2 \tilde{\Lambda}_D^2}{\Lambda_D^2}\right). \tag{B5}$$

Following [60], the differential scattering rate per unit detector mass is

$$\frac{dR}{dE_R} = \frac{\rho_0 v_0}{m_N m_{\rm DM}} \int_{v_{\rm min}(E_R)} d^3v \frac{v}{v_0} f(v; v_e) \frac{d\sigma}{dE_R}, \tag{B6}$$

where $\rho = 0.3$ GeV/cm^3 is the local density of dark matter, and $f(v)$ is the dark matter velocity and velocity distribution function in the lab frame. Introducing a $\Theta(v_{\rm esc} - v)$ to naively cut off the velocity profile above the galactic escape velocity $v_{\rm esc} \approx 500$–600 km/s, we use a simple velocity distribution function,

$$f(v; v_e) \propto (e^{-((\vec{v}-\vec{v}_e)^2/v_0^2)} - e^{-(v_{\rm esc}^2/v_0^2)})\Theta(v_{\rm esc} - |\vec{v} - \vec{v}_e|), \tag{B7}$$

where $v_0 \approx 220$ km/s, and v_e is the Earth's speed in the galactic frame. We use the numerical values reported in [60] for $\vec{v}_e$. For the annual modulation rate, we use

$$\left(\frac{dR}{dE_R}\right)_{\rm modulated} \approx \frac{1}{2}\left(\frac{dR}{dE_R}\bigg|_{\rm June\ 2} - \frac{dR}{dE_R}\bigg|_{\rm Dec\ 2}\right). \tag{B8}$$

To normalize the combination $\alpha_D\epsilon^2$, we fit to the reported DAMA/LIBRA signal, using the combined 0.82 ton-yr exposure [10]. We do this by minimizing a χ^2 function using the 12 half-keVee bins and reported error bars between 2–8 keVee with $10 = 12 - 2$ independent degrees of freedom. The lower and upper ranges of $\alpha_D\epsilon^2$ are taken by scanning over the region with $\chi^2 \leq 16$, and typically differ by a factor of $\sim$10. Our estimate is obtained by taking the geometric mean of the lower and upper values of $\alpha_D\epsilon^2$.

[1] S. W. Barwick *et al.* (HEAT Collaboration), Astrophys. J. **482**, L191 (1997).
[2] O. Adriani *et al.* (PAMELA Collaboration), arXiv:0810.4995.
[3] O. Adriani *et al.*, arXiv:0810.4994.
[4] S. Torii *et al.*, arXiv:0809.0760.
[5] J. Chang *et al.*, Nature (London) **456**, 362 (2008).
[6] M. Aguilar *et al.* (AMS-01 Collaboration), Phys. Lett. B **646**, 145 (2007).
[7] C. Grimani *et al.*, Astron. Astrophys. **392**, 287 (2002).
[8] N. Arkani-Hamed, D. P. Finkbeiner, T. Slatyer, and N. Weiner, Phys. Rev. D **79**, 015014 (2009).
[9] D. Alves, S. R. Behbahani, P. Schuster, and J. G. Wacker, arXiv:0903.3945.
[10] R. Bernabei *et al.*, Int. J. Mod. Phys. D **13**, 2127 (2004).
[11] R. Bernabei *et al.* (DAMA Collaboration), Eur. Phys. J. C **56**, 333 (2008).
[12] D. Tucker-Smith and N. Weiner, Phys. Rev. D **64**, 043502 (2001).
[13] S. Chang, G. D. Kribs, D. Tucker-Smith, and N. Weiner, arXiv:0807.2250.
[14] A. W. Strong *et al.*, Astron. Astrophys. **444**, 495 (2005).
[15] D. P. Finkbeiner and N. Weiner, Phys. Rev. D **76**, 083519 (2007).
[16] B. Batell, M. Pospelov, and A. Ritz, arXiv:0903.0363.
[17] N. Borodatchenkova, D. Choudhury, and M. Drees, Phys. Rev. Lett. **96**, 141802 (2006).
[18] M. J. Strassler and K. M. Zurek, Phys. Lett. B **651**, 374 (2007).
[19] M. J. Strassler, arXiv:hep-ph/0607160.
[20] T. Han, Z. Si, K. M. Zurek, and M. J. Strassler, J. High Energy Phys. 07 (2008) 008.
[21] M. J. Strassler, arXiv:0801.0629.
[22] N. Arkani-Hamed and N. Weiner, J. High Energy Phys. 12 (2008) 104.
[23] M. Baumgart, C. Cheung, J. T. Ruderman, L.-T. Wang, and I. Yavin, arXiv:0901.0283.
[24] T. Hambye, J. High Energy Phys. 01 (2009) 028.
[25] J. F. Gunion, D. Hooper, and B. McElrath, Phys. Rev. D **73**, 015011 (2006).
[26] B. McElrath, Phys. Rev. D **72**, 103508 (2005).
[27] R. Dermisek, J. F. Gunion, and B. McElrath, Phys. Rev. D **76**, 051105 (2007).
[28] J. Galloway, B. McElrath, and J. McRaven, Phys. Lett. B **670**, 363 (2009).
[29] B. Holdom, Phys. Lett. B **178**, 65 (1986).
[30] K. R. Dienes, C. F. Kolda, and J. March-Russell, Nucl. Phys. B **492**, 104 (1997).
[31] S. A. Abel, M. D. Goodsell, J. Jaeckel, V. V. Khoze, and A. Ringwald, J. High Energy Phys. 07 (2008) 124.
[32] D. P. Finkbeiner, Astrophys. J. **614**, 186 (2004).
[33] C. Boehm, D. Hooper, J. Silk, M. Casse, and J. Paul, Phys. Rev. Lett. **92**, 101301 (2004).
[34] Z. Ahmed *et al.* (CDMS Collaboration), Phys. Rev. Lett. **102**, 011301 (2009).
[35] E. Harrison, P. F. and E. Quinn, and R. Helen (*BABAR* Collaboration), *The BABAR Physics Book: Physics at an Asymmetric B Factory, Papers from Workshop on Physics at an Asymmetric B Factory (BABAR Collaboration Meeting), Rome, Italy, 1996; Princeton, NJ, 1997; Orsay, France, 1997; and Pasadena, CA, 1997* (Caltech, Pasadena, 1997).
[36] M. Pospelov, arXiv:0811.1030.
[37] M. Passera, W. J. Marciano, and A. Sirlin, arXiv:0809.4062.
[38] G. W. Bennett *et al.* (Muon $g-2$ Collaboration), Phys. Rev. D **73**, 072003 (2006).
[39] C. Amsler *et al.* (Particle Data Group Collaboration), Phys. Lett. B **667**, 1 (2008).
[40] R. Balest *et al.* (CLEO Collaboration), Phys. Rev. D **51**, 2053 (1995).
[41] B. Aubert (*BABAR* Collaboration), arXiv:0902.2176.
[42] M. Kamionkowski and S. Profumo, Phys. Rev. Lett. **101**, 261301 (2008).
[43] R. Essig, N. Sehgal, and L. E. Strigari, arXiv:0902.4750.
[44] S. Galli, F. Iocco, G. Bertone, and A. Melchiorri, arXiv:0905.0003.
[45] J. F. Gunion, H. E. Haber, G. K. Kane, and S. Dawson, *The Higgs Hunter's Guide* (Westview, Boulder, 2000)
[46] A. Katz and R. Sundrum, arXiv:0902.3271.
[47] C. Cheung, J. T. Ruderman, L.-T. Wang, and I. Yavin, arXiv:0902.3246.
[48] Q.-B. Xie and X.-M. Liu, Phys. Rev. D **38**, 2169 (1988).
[49] R. Schwitters *et al.*, Phys. Rev. Lett. **35**, 1320 (1975).
[50] K. Abe *et al.* (SLD Collaboration), Phys. Lett. B **371**, 149 (1996).
[51] P. V. Chliapnikov, Sov. Phys. Usp. **35**, 441 (1992).
[52] B. Jean-Marie *et al.*, SLAC Report No. SLAC-PUB-1711 1976 (unpublished).
[53] D. M. Asner *et al.*, arXiv:0809.1869.
[54] M. Ahlers, H. Gies, J. Jaeckel, J. Redondo, and A. Ringwald, Phys. Rev. D **77**, 095001 (2008).
[55] M. Ahlers, J. Jaeckel, J. Redondo, and A. Ringwald, Phys. Rev. D **78**, 075005 (2008).
[56] P. D. Serpico and G. G. Raffelt, Phys. Rev. D **70**, 043526 (2004).
[57] M. Davier, S. Eidelman, A. Hocker, and Z. Zhang, Eur. Phys. J. C **27**, 497 (2003).
[58] M. Davier, "Precision Measurement of the $e^+e^- \to \pi^+\pi^-(\gamma)$ Cross-section with the ISR Method," 2008 (unpublished), http://tau08.inp.nsk.su/prog.php.
[59] R. H. Helm, Phys. Rev. **104**, 1466 (1956).
[60] J. D. Lewin and P. F. Smith, Astropart. Phys. **6**, 87 (1996).